J|A|C|S ARTICLES

Published on Web 04/07/2009

Bimetallic Effects for Enhanced Polar Comonomer Enchainment Selectivity in Catalytic Ethylene Polymerization

Brandon A. Rodriguez, Massimiliano Delferro, and Tobin J. Marks*

Department of Chemistry, Northwestern University, Evanston, Illinois 60208-3113

Received July 3, 2008; E-mail: t-marks@northwestern.edu

Abstract: The synthesis and characterization of the bimetallic 2,7-di-[(2,6-diisopropylphenyl)imino]-1,8-naphthalenediolato group 10 metal polymerization catalysts {[Ni(CH_3)]$_2$[1,8-(O)$_2$$C_{10}H_4$-2,7-[CH=N(2,6-^{i}Pr$_2$$C_6H_3$)](P$Me_3$)$_2$} and {[Ni(1-naphthyl)]$_2$[1,8-(O)$_2$$C_{10}H_4$-2,7-[CH=N(2,6-^{i}Pr$_2$$C_6H_3$)](P$Ph_3$)$_2$} [**FI^2-Ni$_2$(PR$_3$)$_2$**] are presented, along with the synthesis and characterization of the mononuclear analogues {Ni(CH_3)[3-^{t}Bu-2-(O)C_6H_3CH=N(2,6-^{i}Pr$_2$$C_6H_3$)](P$Me_3$)$_3$} and {Ni(1-naphthyl)[3-^{t}Bu-2-(O)C_6H_3CH=N(2,6-^{i}Pr$_2$$C_6H_3$)](P$Ph_3$)$_3$} [**FI-Ni (PR$_3$)**]. Monometallic Ni catalysts were also prepared by functionalizing one ligation center of the bimetallic ligand with a trimethylsilyl group (TMS), yielding {Ni(CH_3)[1,8-(O)(TMSO)$C_{10}H_4$-2,7-[CH=N(2,6-^{i}Pr$_2$$C_6H_3$)](P$Me_3$)$_3$} [**TMS-FI^2-Ni(PMe$_3$)$_3$**]. The **FI^2-Ni$_2$** catalysts exhibit significant increases in ethylene homopolymerization activity versus the monometallic analogues, as well as increased branching and methyl branch selectivity, even in the absence of a Ni(cod)$_2$ cocatalyst. Increasing ethylene concentrations significantly suppress branching and alter branch morphology. **FI^2-Ni$_2$**-mediated copolymerizations with ethylene + polar-functionalized norbornenes exhibit a 4-fold increase in comonomer incorporation versus **FI-Ni**, yielding copolymers with up to 10% norbornene copolymer incorporation. **FI^2-Ni$_2$**-catalyzed copolymerizations with ethylene + methylacrylate or methyl methacrylate incorporate up to 11% acrylate comonomer, while the corresponding mononuclear **FI**−**Ni** catalysts incorporate negligible amounts. Furthermore, the **FI^2-Ni$_2$**-mediated polymerizations exhibit appreciable polar solvent tolerance, turning over in the presence of ethyl ether, acetone, and even water. The mechanism by which the present cooperative effects take place is investigated, as is the nature of the copolymer microstructures produced.

1. Introduction

Over the past few years much research attention has focused on discovering more efficient and selective homogeneous catalytic processes made possible by cooperative effects between proximate active centers in multinuclear metal complexes.[1] In some cases, these complexes mimic the capabilities of enzymes in enforcing conformational control and preorganization to promote selectivity.[1] Research from this laboratory in the field of single-site[2] bimetallic olefin polymerization catalysis has shown that in group 4 constrained geometry[3,4] and aryloxyiminato[5] catalytic systems exhibit increased activity, branch formation, and comonomer enchainment versus their mononuclear analogues (Chart 1). The origin of these effects is proposed to include non-negligible comonomer secondary binding to weakly

(1) (a) Esswein, A. J.; Veige, A. S.; Piccoli, P. M. B.; Schultz, A. J.; Nocera, D. G. *Organometallics* **2008**, *27*, 1073–1083. (b) Li, C.; Chen, L.; Garland, M. *J. Am. Chem. Soc.* **2007**, *129*, 13327–13334. (c) Weng, Z.; Teo, S.; Liu, Z.; Hor, T. S. A. *Organometallics* **2007**, *26*, 2950–2952. (d) Sammis, G. M.; Danjo, H.; Jacobsen, E. N. *J. Am. Chem. Soc.* **2004**, *126*, 9928–9929. (e) Collman, J. P.; Boulatov, R.; Sunderland, C. J.; Fu, L. *Chem. Rev.* **2004**, *104*, 561–588. (f) Krishnan, R.; Voo, J. K.; Riordan, C. G.; Zahkarov, L.; Rheingold, A. L. *J. Am. Chem. Soc.* **2003**, *125*, 4422–4423. (g) Moore, D. R.; Cheng, M.; Lobkovsky, E. B.; Coates, G. W. *J. Am. Chem. Soc.* **2003**, *125*, 11911–11924. (h) Trost, B. M.; Mino, T. *J. Am. Chem. Soc.* **2003**, *125*, 2410–2411. (i) Jacobsen, E. N. *Acc. Chem. Res.* **2000**, *33*, 421–431. (j) Molenveld, P.; Engbersen, J. F. J.; Reinhoudt, D. N. *Chem. Soc. Rev.* **2000**, *29*, 75–86. (k) Konsler, R. G.; Karl, J.; Jacobsen, E. N. *J. Am. Chem. Soc.* **1998**, *120*, 10780–10781. (l) Molenveld, P.; Kapsabelis, S.; Engbersen, J. F. J.; Reinhoudt, D. N. *J. Am. Chem. Soc.* **1997**, *119*, 2948–2949. (m) Mathews, R. C.; Howell, D. H.; Peng, W.-J.; Train, S. G.; Treleaven, W. D.; Stanley, G. G. *Angew. Chem., Int. Ed. Engl.* **1996**, *35*, 2253–2256. (n) Sawamura, M.; Sudoh, M.; Ito, Y. *J. Am. Chem. Soc.* **1996**, *118*, 3309–3310.

(2) For recent reviews of single-site olefin polymerization, see: (a) Amin, S. B.; Marks, T. J. *Angew. Chem., Int. Ed.* **2008**, *47*, 2006–2025. (b) Marks, T. J. *Proc. Natl. Acad. Sci. U.S.A.* **2006**, *103*, 15288–15354, and contributions therein (special feature on polymerization). (c) Suzuki, N. *Top. Organomet. Chem.* **2005**, *8*, 177–216. (d) Alt, H. G. *Dalton Trans.* **2005**, *20*, 3271–3276. (e) Kaminsky, W. J. *Polym. Sci. Polym. Chem.* **2004**, *42*, 3911–3921. (f) Wang, W.; Wang, L. *J. Polym. Mater.* **2003**, *20*, 1–8. (g) Delacroix, O.; Gladysz, J. A. *Chem. Commun.* **2003**, *6*, 665–675. (h) Kaminsky, W.; Arndt-Rosenau, M. *Applied Homogeneous Catalysis with Organometallic Compounds*, 2nd ed.; Wiley-VCH Verlag GmbH: Weinheim, Germany, 2002. (i) Lin, S.; Waymouth, R. M. *Acc. Chem. Res.* **2002**, *35*, 765–773. (j) Chen, E. Y-X.; Marks, T. J. *Chem. Rev.* **2000**, *100*, 1391–1434. (k) Gladysz, J. A. *Chem. Rev.* **2000**, *100*,and contributions therein. (l) Schweier, G.; Brintzinger, H.-H. *Macromol. Symp.* **2001**, *173*, 89–103. (m) Kaminsky, W. *Catal. Today* **2000**, *62*, 23–34. (n) Kaminsky, W. *Adv. Catal.* **2001**, *46*, 89–159.

(3) (a) Review: Li, H.; Marks, T. J. *Proc. Natl. Acad. Sci. U.S.A.* **2006**, *103*, 15295–15302, and references therein. (b) Li, H.; Stern, C. L.; Marks, T. J. *Macromolecules* **2005**, *38*, 9015–9027. (c) Li, H.; Li, L.; Schwartz, D. J.; Stern, C. L.; Marks, T. J. *J. Am. Chem. Soc.* **2005**, *127*, 14756–14768. (d) Li, H.; Li, L.; Marks, T. J. *Angew. Chem., Int. Ed.* **2004**, *43*, 4937–4940. (e) Guo, N.; Li, L.; Marks, T. J. *J. Am. Chem. Soc.* **2004**, *126*, 6542–6543. (f) Li, H.; Li, L.; Marks, T. J.; Liable-Sands, L.; Rheingold, A. L. *J. Am. Chem. Soc.* **2003**, *125*, 10788–10789.

(4) (a) Guo, N.; Stern, C. L.; Marks, T. J. *J. Am. Chem. Soc.* **2008**, *130*, 2246–2261. (b) Amin, S.; Marks, T. J. *J. Am. Chem. Soc.* **2007**, *129*, 2938–2953. (c) Amin, S.; Marks, T. J. *J. Am. Chem. Soc.* **2006**, *128*, 4506–4507. (d) Guo, N.; Li, L.; Marks, T. J. *J. Am. Chem. Soc.* **2004**, *126*, 6542–6543.

10.1021/ja900257k CCC: $40.75

Chart 1. Group 4 Mononuclear and Bimetallic Olefin Polymerization Catalysts

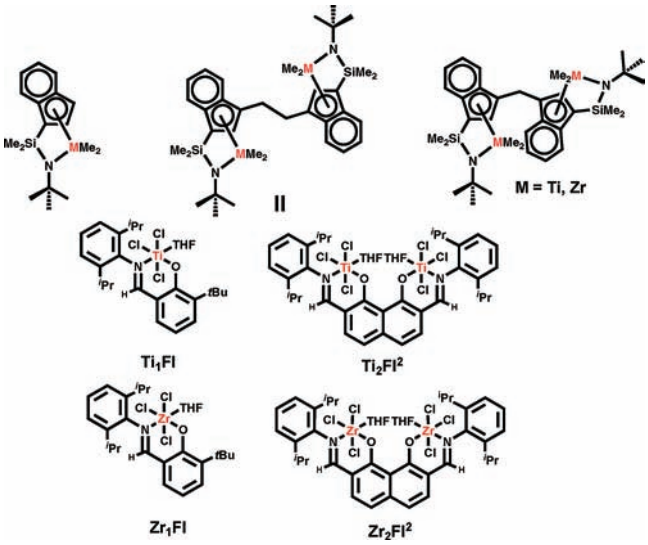

basic groups on the olefin which modifies relative chain transfer rates and facilitates comonomer enchainment at the second, proximate metal center, as shown in **A**.[4−6] An excellent example of this is observed in polystyrene homopolymerizations with the binuclear CGC catalysts[4] (**II**). Here binuclear cooperative Ti···arene interactions significantly enhance styrene homopolymerization rates, modify enchainment regioselectivity, and greatly increase comonomer enchainment selectivity (e.g., **B**).[4] The group 4 studies indicate that the degree of cooperativity between the two catalytic centers in these catalysts scales roughly inversely with intermetallic distance.[3]

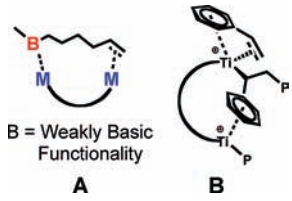

Although very high olefin polymerization and copolymerization activities can be achieved with the group 4 catalysts, be it via CGC ancillary ligation or otherwise, the electrophilicity and polymerization activity of these metal centers is greatly depressed in the presence of polar comonomers or polar solvents. Desirable properties arising from the incorporation of polar functionalities into polyolefins include precise control over polymer characteristics such as mechanical toughness, rheology, and surface functionalization properties,[7] while the ability of the catalyst to withstand polar solvents allows bypassing the need for rigorous drying of the polymerization solvent. In order to develop single-site catalysts more compatible with polar functionalities, our attention turned from the oxophilic group 4 metals toward catalyst systems with more electron-rich catalyst centers, such as the group 10 metals. The cationic and neutrally charged group 10 systems pioneered by Brookhart, Johnson, Ittel, et al.[8,9] (e.g., **C** and **D**) demonstrate that coordinative enchainment of polar monomers such as acrylates is indeed possible in highly branched polyethylenes or polypropylenes, where the enchained acrylate units predominately cap the branch ends. Contemporaneously, Grubbs et al.[10,11] demonstrated that neutrally charged Ni catalytic systems such as **E** mediate ethylene copolymerization with functionalized norbornenes while producing very highly branched polymers. Some density of controlled branching in polyolefins is desirable to depress the glass transition and melting temperatures, thus enhancing processability.[8−12] Also of note is that the group 10 catalysts are active in the presence of polar solvent additives, with only minor reductions in activity,[11] bypassing the need for hyperpurification of polymerization media. Although polar comonomers can be introduced into polyolefins via radical and other polymerization methods, single-site catalysts offer the attraction of greater control over polymer microstructure, polydispersity, and tunability of comonomer content.[8−12] The ability to effect these polymerizations via a coordinative/insertive pathway instead of the typically used free-radical processes also circumvents the need for expensive reactors and extremely high pressures.[8,13] The above Ni catalyst systems are capable of introducing over 50 branches/1000 C into the polymer chain, yielding polymers with lower melting points than those produced by their group 4 counterparts, although typically with lower molecular weight. The group 10 systems typically incorporate 2−4 mol % of functionalized and nonfunctionalized norbornenes, further depressing the melting point and serving as an interesting starting point for determining what comonomers can be incorporated and to what extent.

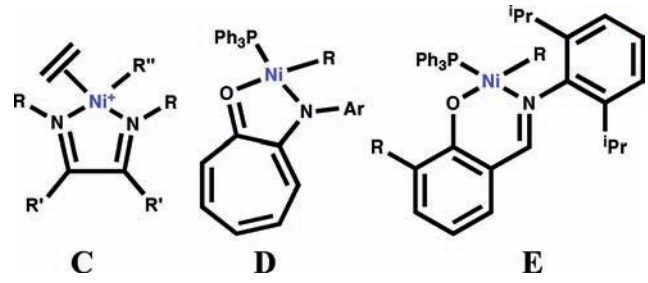

The above results raise the intriguing question of whether the advantageous characteristics of binuclear polymerization catalysts (Chart 1) might be applied to group 10 catalytic

(5) (a) Salata, M. R.; Marks, T. J. *J. Am. Chem. Soc.* **2008**, *130*, 12–13. (b) Salata, M. R.; Marks, T. J. *Macromolecules* **2009**, *42*, 1920–1933.
(6) DFT computation: (a) Motta, A.; Fragalá, I.; Marks, T. J. *Proceedings 13th ISHHC*; 13th ISHHC; Berkeley CA; July, 2000, Abstract 47. (b) Motta, A.; Fragalá, I.; Marks, T. J. *J. Am. Chem. Soc.* **2009**, *131*, 3974–3984.
(7) (a) Yanjarappa, M. J.; Sivaram, S *Prog. Polym. Sci.* **2002**, *27*, 1347, and references therein. (b) Boffa, L. S.; Novak, B. M *Chem. Rev.* **2000**, *100*, 1479, and references therein.
(8) (a) Domski, G. J.; Rose, J. M.; Coates, G. W.; Bolig, A. D.; Brookhart, M. *Prog. Polym. Sci.* **2007**, *32*, 30–92. (b) McCord, E. F.; McLain, S. J.; Nelson, L. T. J.; Ittel, S. D.; Tempel, D.; Killian, C. M.; Johnson, L. K.; Brookhart, M *Macromolecules* **2007**, *40*, 410–420. (c) Zhang, L.; Brookhart, M.; White, P. S. *Organometallics* **2006**, *25*, 1868–1874. (d) Jenkins, J. C.; Brookhart, M. J. *J. Am. Chem. Soc.* **2004**, *126*, 5827–5842. (e) Gibson, V. C.; Spitzmesser, S. K. *Chem. Rev.* **2003**, *103*, 283–316. (f) Ittel, S. D.; Brookhart, M. *Chem. Rev.* **2000**, *100*, 1169–1203. (g) Desjardins, S. Y.; Cavell, K. J.; Hoare, J. L.; Skelton, B. W.; Sobolev, A. N.; White, A. W.; Keim, W. *J. Organomet. Chem.* **1997**, *544*, 163. (h) Kurtev, K.; Tomov, A. *J. Mol. Catal.* **1994**, *88*, 141. (i) Klabunde, U.; Ittel, S. D. *J. Mol. Catal.* **1987**, *41*, 123. (j) Klabunde, U.; Mülhaupt, R.; Herskovitz, T.; Janowicz, A. H.; Calabrese, J.; Ittel, S. D. *J. Polym. Sci., Part A: Polym. Chem.* **1987**, *25*, 1989.
(9) Hicks, F. A.; Brookhart, M. *Organometallics* **2001**, *20*, 3217–3219.
(10) Connor, E. F.; Younkin, T, R.; Henderson, J. I.; Hwang, S.; Grubbs, R. H.; Roberts, W. P.; Litzau, J. J. *J. Polym. Sci., Part A: Polym. Chem.* **2002**, *40*, 2842–2854.

Chart 2. Group 10 Mononuclear and Bimetallic Olefin Polymerization Catalysts R = CH_3 and Naphthyl

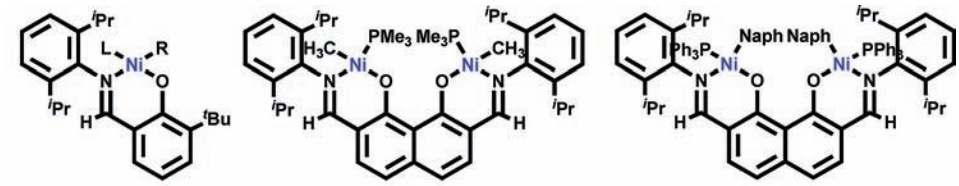

systems. Attractions include the possibility of modifying polymerization rates and selectivites while enhancing selectivity for monomers having basic substituents, as in structures **A** and **B** above, and tolerance to polar media, which is not possible for the group 4 catalysts. A group 10 binuclear catalyst would also allow probing the full scope of the bimetallic cooperativity effects first demonstrated with the aforementioned group 4 catalysts by providing a broader spectrum of polymerization conditions and monomers to be explored.

We recently communicated[14] the synthesis of binuclear naphthyloxydiiminato Ni(II) catalysts **FI²-Ni₂-(PPh₃)₂** and **FI²-Ni₂-(PMe₃)₂** in which the rigid ligation ensures that the metal centers are bound in close spatial proximity (Chart 2). In initial ethylene homopolymerizations mimicking the reaction conditions of previous monometallic group 10 work, the **FI²-Ni₂** systems exhibited a doubling in catalytic activity for ethylene homopolymerizations, introduced significantly more alkyl branches than our mononuclear **FI** catalysts, and exhibited a strong selectivity for methyl-only branch formation (>99%). Intriguing preliminary binuclear copolymerization effects were observed with norbornene. In the present contribution, we present a detailed study of **FI²-Ni₂** synthetic, solid-state and solution structural, and olefin polymerization catalytic chemistry. Using the monometallic Ni analogues as controls, we show that (1) Ethylene hompolymerizations in the presence of **FI²-Ni₂** exhibit significantly increased activity to produce different product microstructures than the mononuclear **FI-Ni** catalysts. (2) This enhanced activity is maintained in the presence of polar cosolvents, while concurrently retaining the selectivity for large branch densities. (3) Substantial cooperativity effects are operative in **FI²-Ni₂**-mediated copolymerizations of ethylene with functionalized norbornenes, with a 4× enhancement in enchainment selectivity, and (4) Ethylene copolymerizations with normally unresponsive acrylate esters achieve up to 11% comonomer incorporation in reactions catalyzed by **FI²-Ni₂** versus negligible enchainment by **FI-Ni** catalysts. As supported by structural, in situ NMR spectroscopic, and product polymer microstructure studies, these results are in accord with substantial Ni···Ni mediated cooperative effects in the enchainment process.

2. Experimental Section

2.1. Materials and Methods. All manipulations of air-sensitive materials were performed with rigorous exclusion of oxygen and moisture in flamed Schlenk-type glassware on a dual manifold Schlenk line, or interfaced to a high-vacuum line (10^{-5} Torr), or in a nitrogen-filled Vacuum Atmospheres glovebox with a high capacity recirculator (<1 ppm O_2). Argon and ethylene (Matheson, polymerization grade) were purified by passage through a supported MnO oxygen-removal column and an activated Davison 4 A molecular sieve column. Ether solvents were purified by distillation from Na/K alloy/benzophenone ketyl. Hydrocarbon solvents (*n*-pentane and toluene) were dried using activated alumina columns according to the method described by Grubbs, and were additionally vacuum-transferred from Na/K alloy immediately before vacuum line manipulations. All solvents for high-vacuum line manipulations were stored *in vacuo* over Na/K alloy in Teflon-valve sealed bulbs. Deuterated solvents were obtained from Cambridge Isotope Laboratories (all ≥99 atom %D), were freeze pump−thaw degassed, dried over Na/K alloy and were stored in resealable flasks. Other nonhalogenated solvents were dried over Na/K alloy, and halogenated solvents were distilled from CaH_2 and stored over activated Davison 4 A molecular sieves. The reagents *trans*-[NiMeCl(PMe_3)$_2$], *trans*-[Ni(1-naphthyl)Cl(PPh_3)$_2$], 2,7-di(2,6-diisopropylphenyl)imino-1,8-dihydroxynaphthalene, salicylaldimine and salicylaldiminate sodium salt were prepared according to literature procedures.[3a] [Ni(cod)$_2$] (cod = 1,5-cyclooctadiene) was purchased from Aldrich. The synthesis of monometallic and bimetallic

(11) (a) Waltman, A.; Younkin, T.; Grubbs, R. H. *Organometallics* **2004**, *23*, 5121–5123. (b) Connor, E. F.; Younkin, T, R.; Henderson, J. I.; Hwang, S.; Grubbs, R. H.; Roberts, W. P.; Litzau, J. J. *J. Polym. Sci., Part A: Polymer Chem.* **2002**, *40*, 2842–2854. (c) Younkin, T. R.; Connor, E. F.; Henderson, J. I.; Friedrich, S. K.; Grubbs, R. H.; Bansleben, D. A. *Science* **2000**, *287*, 460. (d) Wang, C.; Friedrich, S. K.; Younkin, T. R.; Li, R. T.; Grubbs, R. H.; Bansleben, D. A.; Day, M. W. *Organometallics* **1998**, *17*, 3149. (e) Connor, E. F.; Younkin, T. R.; Henderson, J. I.; Waltman, A. W.; Grubbs, R. H. *Chem. Commun.* **2003**, 2272–2273.

(12) (a) Cotts, P. M.; Guan, Z.; McCord, E. F.; McLain, S. *Macromolecules* **2000**, *33*, 6945. (b) Kang, M.; Sen, A. *Organometallics* **2005**, *24*, 3508–3515.

(13) (a) Hu, T.; Li, Y.; Li, Y.; Hu, N. *J. Polym. Sci., Part A: Polymer Chem.* **2006**, *253*, 155–164. (b) Li, X.; Li, Y.; Li, Y.; Chen, Y.; Hu, N. *Organometallics* **2005**, *24*, 2502–2510. (c) Sujith, S.; Joe, D. J.; Na, S. J.; Park, Y.; Choi, C. H.; Lee, B. Y. *Macromolecules* **2005**, *38*, 10027–10033. (d) Jenkins, J. C.; Brookhart, M. *J. Am. Chem. Soc.* **2004**, *126*, 5824–5827. (e) JohnsonL.; Bennett, A.; Dobbs, K.; Hauptman, E.; Ionkin, A.; Ittel, S.; McCord, E.; McLain, S.; Radzewich, C.; Yin, Z.; Wang, L.; Wang, Y.; Brookhart, M. *PMSE Preprints 86*; 223rd National Meeting of the American Chemical Society, Division of Polymeric Materials: Science and Engineering; Orlando, FL; April 7−11, 2002, American Chemical Society: Washington, D.C., 2002; p 319. (f) Wang, L.; Hauptman, E.; Johnson, L. K.; McCord, E. F.; Wang Y. Ittel, S. D.; Radzewich, C. E.; Kunitsky, K.; Ionkin, A. S. *PMSE Preprints 86*; 223rd National Meeting of the American Chemical Society, Division of Polymeric Materials: Science and Engineering; Orlando, FL; April 7−11, 2002, American Chemical Society: Washington, D.C., 2002; p 319. (g) Johnson, L., Bennett, A.; Dobbs, K.; Haupman, A.; Ionkin, A.; Ittel, S.; McCord, E.; McLain, S.; Radsewich, C.; Yin, Z.; Wang, L.; Wang, Y.; Brookhart, M. *PMSE Preprints 86*; 223rd National Meeting of the American Chemical Society, Division of Polymeric Materials: Science and Engineering; Orlando, FL; April 7−11, 2002, American Chemical Society: Washington, D.C., 2002; p 319. (h) Johnson, L.; Bennett, A.; Dobbs, K., HauptmanE.; Ionkin, A.; Ittel, S.; McCord, E.; McLain, S.; Radzewich, C.; Yin, Z.; Wang, L.; Wang, Y.; Brookhart, M. *PMSE Preprints 86*; 223rd National Meeting of the American Chemical Society, Division of Polymeric Materials: Science and Engineering; Orlando, FL; April 7−11, 2002, American Chemical Society: Washington, D.C., 2002; p 319. (i) McCord, E. F.; McLain, S. J.; Nelson, L. T. J.; Arthur, S. D.; Coughlin, E. B.; Ittel, S. D.; Johnson, L. K.; Tempel, D.; Killian, C. M.; Brookhart, M. *Macromolecules* **2001**, *34*, 362–371. (j) Bauers, F. M.; Mecking, S. *Macromolecules* **2001**, *34*, 1165–1171.

(14) Rodriguez, B. A.; Delferro, M.; Marks, T. J. *Organometallics* **2008**, *27*, 2166–2168.

Table 1. Crystallographic Data and Structure Refinement Details for Complexes $(FI^2Ni)_2$ and $(FI^2Ni_2PMe_3)\cdot PMe_3$

	$(FI^2Ni)_2$	$(FI^2Ni_2PMe_3)\cdot PMe_3$
empirical formula	$C_{64}H_{84}N_4O_4Ni_2$	$C_{41}H_{55}N_2O_2PNi_2$
FW	1429.00	754.27
temperature, K	173(2)	173(1)
wavelength, Å	0.71703	0.71703
crystal system	triclinic	triclinic
space group	$P\bar{1}$	$P\bar{1}$
a, Å	9.5250	11.9810
b, Å	11.4900	13.7930
c, Å	16.8800	16.2210
α, deg	101.216	78.109
β, deg	96.502	72.759
γ, deg	105.244	83.782
V, Å^3	1721.7(7)	2502.2(3)
Z	4	2
D_{calcd}, g cm^{-3}	1.422	1.261
$F(000)$	1429	1656
crystal size, mm^3	0.02 × 0.02 × 0.02	0.10 × 0.16 × 0.28
μ, cm^{-1}	0.650	0.595
θ range (deg)	4.03−20.84	2.06−30.00
rflns collected	90633	146770
rflns unique	4020 [R(int) = 0.0577]	11819 [R(int) = 0.0553]
data/restraints/parameters	4020/0/460	11819/0/460
final R indices [$I > 2\sigma(I)$]	R1[a] = 0.0592, wR2[b] = 0.1611	R1[a] = 0.0570, wR2[b] = 0.1422
R indices (all data)	R1[a] = 0.0793, wR2[b] = 0.1784	R1[a] = 0.0746, wR2[b] = 0.1664

[a] $R1 = \Sigma||F_o| - |F_c||/\Sigma|F_o|$. [b] $wR2 = [\Sigma[w(F_o^2 - F_c^2)^2]/\Sigma[w(F_o^2)^2]]$.

catalysts **FI-Ni-A**, **FI-Ni-B**, **FI^2-Ni$_2$-A**, **FI^2-Ni$_2$-B**, and **FI^2(TMS)-Ni** was carried out as previously reported.[14]

2.2. Physical and Analytical Measurements. NMR spectra, including TOCSY, COSY, and HSQC, were recorded on Bruker AVANCEIII (FT, 600 MHz, ^{1}H; 150 MHz ^{13}C), Varian ^{UNITY}Inova-500 (FT, 500 MHz, ^{1}H; 125 MHz, ^{13}C), ^{UNITY}Inova-400 (FT, 400 MHz, ^{1}H; 100 MHz, ^{13}C) and Mercury-400 (FT 400 MHz, ^{1}H; 100 MHz, ^{13}C; 162 MHz, ^{31}P) instruments. Chemical shifts (δ) for ^{1}H and ^{13}C spectra were referenced using internal solvent resonances and are reported relative to tetramethylsilane. Chemical shifts (δ) for ^{31}P spectra are reported relative to an external 85% H_3PO_4 standard. NMR experiments on air-sensitive samples were conducted in Teflon valve-sealed sample tubes (J.Young). Elemental analyses were performed by Midwest Microlab, Indianapolis, Indiana. ^{1}H and ^{13}C NMR spectra of polymers were collected in either 1,1,2,2-tetrachloroethane-d_2 at 130 °C and $CDCl_3$ at 25 °C. In ethylene polymerizations, spectral assignments were made as described in the literature,[15] with extra care taken to ensure that peak widths of the methyl branch signal were representative of the true branch density. In copolymerizations, the additional product resonances were assigned to the corresponding comonomer functional groups as described in the literature.[11,15] In each of the copolymerizations, ^{13}C NMR integration of the comonomer resonances versus those in the PE backbone was used to determine the density of incorporation. Signals were assigned according to the literature for the polyethylene part.[15] FTIR spectra were collected on a Bio-Rad FTS spectrophotometer (KBr pellet). Melting temperatures of polymers were measured by DSC (DSC 2920, TA Instruments, Inc.) from the second scan with a heating rate of 10 °C/min. GPC-RI measurements were performed on a Polymer Laboratories PL-GPC 220 instrument using 1,2,4-trichlorobenzene solvent (stabilized with 125 ppm BHT) at 150 °C. A set of three PLgel 10 μm mixed columns was used. Samples were prepared at 160 °C. GPC-UV measurements were performed on a Waters GPC 484 instrument using chloroform at 35 °C and two linear 500 mm × 10 mm columns. Molecular weights determined by GPC used narrow polystyrene standards and are not corrected. NMR, DSC, GPC-RI and GPC-UV measurements were performed as explained above, on both product copolymers and on control physical mixtures of the corresponding homopolymers.

2.3. X-ray Crystallography. Crystals of $(FI^2Ni)_2$ and $(FI^2Ni_2PMe_3)\cdot PMe_3$ were grown by slow diffusion of hexane into ethyl ether solutions under a nitrogen atmosphere. Intensity data were collected at 173 K on a Bruker AXS Smart 1000[16] single crystal diffractometer equipped with an area detector using a graphite monochromatic Mo Kα radiation (λ = 0.71073 Å). Crystallographic and experimental details of the structures are summarized in Table 1. An empirical absorption correction was applied to the data. The structures were solved by direct methods and refined by full-matrix least-squares procedures (based on F_o^2),[17] first with isotropic thermal parameters and then with anisotropic thermal parameters in the last cycles of refinement for all the non-hydrogen atoms. The hydrogen atoms were introduced into the geometrically calculated positions and refined riding on the corresponding parent atoms.

2.4. Synthesis of {[2-(*tert*-Butyl)-6-(2,6-diisopropylphenyl)-imino]phenolato}(*n*-butyl)-(triphenylphosphine)Ni(II) and in Situ NMR Studies. A solution of the appropriate salicylaldiminate sodium salt in toluene (30 mL) was added dropwise at −78 °C to a stirring solution of *trans*-$[NiCl_2(PPh_3)_2]$ (in toluene (25 mL). After stirring for 4 h, two equivalents of *n*-BuLi (2.5M) was added dropwise and the mixture allowed to stir at −78 °C for an additional 4 h. The resulting salt was filtered off via cannula and the thermally unstable dinickel complex was dried under vacuum at 0 °C. The dinickel complex was then loaded into an NMR tube along with

(15) (a) Assay procedure from: Gates, D. P.; Svejda, S. A.; Onate, E.; Killian, C. M.; Johnson, L. K.; White, P. S.; Brookhart, M *Macromolecules* **2000**, *33*, 2320. (b) Polyethylene methyl branching densities were determined by ^{1}H NMR spectroscopy using the ratio of the integral of methyl groups to the overall number of carbons (methyl + methylene + methine),[15a] and are reported as branches per 1000 carbons. (c) Chen, Q.; Yu, J; Huang, J *Organometallics* **2007**, *26*, 617–625. (d) Hu, T.; Tang, L.; Li, X.; Li, Y.; Hu, N *Organometallics* **2005**, *24*, 2628–2632. (e) Zhang, D.; Jin, G. *Organometallics* **2003**, *22*, 2851–2854. (f) Liu, W.; Ray, D. G., III; Rinaldi, P. L. *Macromolecules* **1999**, *32*, 3817–3819.

(16) Jurkiewicz, A.; Eilberts, N. W.; Hsieh, E. T. *Macromolecules* **1999**, *32*, 5471–5476.

(17) (a) *SAINT Software Users Guide, Version 6.0*; Bruker Analytical X-ray Systems: Madison, WI, 1999. (b) Sheldrick, G. M., *SADABS*, Bruker Analytical X-ray Systems, Madison, WI, 1999. (c) Sheldrick, G. M., *SHELXL-97, Program for Crystal Structure Refinement*; University of Göttingen: Germany, 1997.

Scheme 1. Synthesis of Binuclear Catalysts **FI²-Ni₂-A** and **FI²-Ni₂-B**, and Mononuclear **FI²(TMS)-Ni** Catalysts

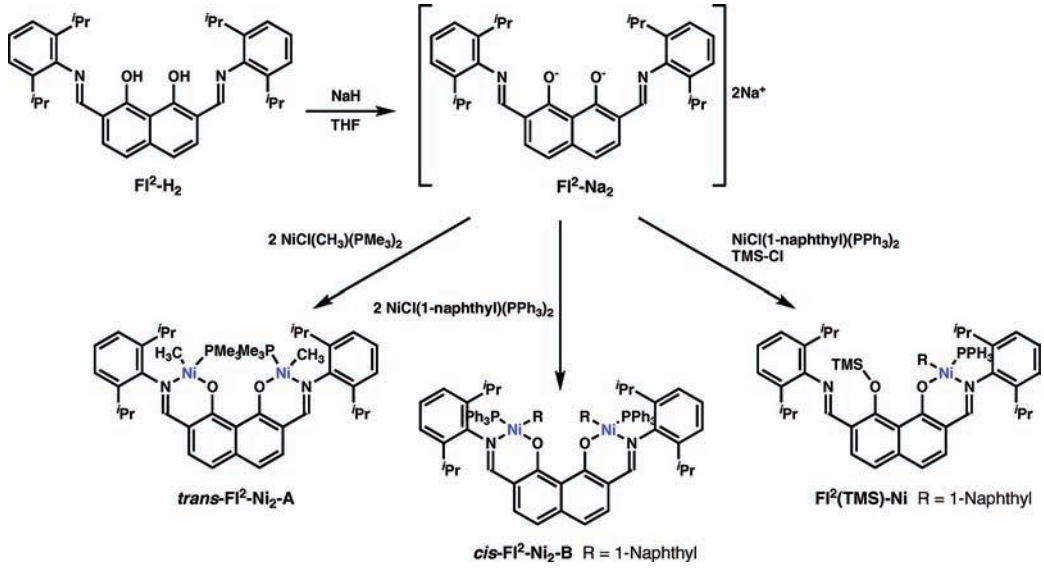

two equivalents of $Ni(cod)_2$ and dissolved in d_8-toluene, all while being kept in a dewar filled with dry ice. Due to the thermal instability of the complex, the NMR probe was cooled to −80 °C beforehand. Spectra were then collected on the Varian ^{UNITY}Inova-400 (FT, 400 MHz, ^{1}H) spectrometer over the temperature range −80 to −20 °C to investigate the nature of the alkyls formed and any agostic interactions.

2.5. General Procedure for Ethylene Polymerization by Ni Catalysts. A 200 mL glass pressure vessel (dried in a 120 °C oven overnight prior to use) was equipped with a large magnetic stir bar, and was heated to the required temperature in an oil bath, with the temperature monitored by thermocouple. At no time was the temperature allowed to deviate more than 2 °C. Next, 25 mL of toluene was injected via syringe into the reactor and the reactor was pressurized with ethylene to 1.0 atm. For trials without cocatalyst, 20 μmol of catalyst solution was then injected, and the pressure brought to 7.0 atm for 2 h with rapid stirring. For cocatalyst-activated trials, a solution of 10 μmol of catalyst in $[Ni(cod)_2]$ was also injected, after which the pressure was increased to 7.0 atm and rapid stirring maintained for 40 min. After the desired run time, the reactor was vented, and the reaction mixture was quenched with 10% HCl in ethanol. The precipitated polymer was stirred overnight, collected by filtration, washed with ethanol, and dried under vacuum at 80 °C overnight.

2.6. General Procedure for Ethylene Polymerization by Ni Catalysts in Polar Solvents. A 200 mL glass pressure vessel (dried in a 120 °C oven overnight prior to use) was equipped with a large magnetic stir bar and heated to the required temperature in an oil bath. Next, 25 mL of toluene was injected into the reactor along with 1500 equiv of the desired rigorously degassed polar solvent additive. The reactor was then pressurized with ethylene to 1.0 atm. Ten micromoles of catalyst solution was then injected and the pressure brought to 7.0 atm for 1 h with rapid stirring. After the desired run time, the reactor was vented, and the reaction mixture was quenched with 10% HCl in ethanol. The precipitated polymer was stirred overnight, collected by filtration, washed with ethanol, and dried under vacuum at 80 °C overnight.

2.7. General Procedure for Ethylene Copolymerization by Ni Catalysts with Acrylates or Functionalized Norbornenes. A 200 mL glass pressure vessel (dried in a 120 °C oven overnight prior to use) was equipped with a large magnetic stir bar and heated to the required temperature in an oil bath. Next, 25 mL of toluene was injected via syringe into the reactor along with 225 equiv of the desired polar comonomer. The reactor was then pressurized with ethylene to 1.0 atm, 20 μmol of catalyst solution was then injected, and the pressure brought to 7.0 atm for 1.5 h with rapid stirring. After the desired run time, the reactor was vented, and the reaction mixture was quenched with 10% HCl in ethanol. The precipitated polymer was stirred overnight, collected by filtration, washed with ethanol, and dried under vacuum at 80 °C overnight.

3. Results

The goal of this study was to explore the scope and mechanism of Ni center−Ni center cooperative enchainment effects in polymerizations mediated by binuclear **FI²-Ni₂**-derived catalysts. This included defining the scope of this cooperativity in ethylene homopolymerizations and in ethylene copolymerizations with polar functionalized norbornenes and acrylates. Here rigorous copolymer microstructure analysis is carried out to differentiate copolymers from mixtures of the corresponding homopolymers. Ethylene homopolymerizations were also carried out in the presence of polar additives to assess the stability of the binuclear cooperativity effects in the presence of coordinating and protic media. Finally, the pathway by which this cooperativity takes place is explored by means of product polymer microstructure analysis, and structural characterization of the catalytic species in the solid state and in solution via in situ low-temperature NMR spectroscopic studies.

3.1. Synthesis and Characterization of Bimetallic Catalysts. The sodium salt of ligand **FI²-H₂**[2] was obtained by treating 2,7-di(2,6-diisopropylphenyl)imino-1,8-dihydroxy-naphthalene[1,3] with NaH in THF. The bimetallic catalysts **FI²-Ni₂-A** and **FI²-Ni₂-B** were then prepared as shown in Scheme 1. All new compounds were characterized by standard analytical and spectroscopic techniques (See Experimental for details). The imine protons in the **FI²-Ni₂-A** ^{1}H NMR spectrum exhibit a characteristic $J_{PH} \approx 9$ Hz, corresponding to PMe_3 coordination *trans* to the ketimine (confirmed by ^{1}H NOESY and ^{1}H COSY). Close proximity of the Ni-CH_3 group and the methyls of one ^{i}Pr group is also detected in the NOESY spectrum. In contrast, $J_{PH} \approx 6$ Hz and the ^{1}H NOESY spectrum indicate *cis*-PPh_3 binding[8] in **FI²-Ni₂-B** (See Supporting Information for these spectra). The ^{1}H-decoupled ^{31}P singlets in both complexes are consistent with the proposed **FI²-Ni₂-A** and **FI²-Ni₂-B** symmetries. Upon standing at elevated temperatures (≥35°), the presence of free phosphine is also detected in the ^{31}P NMR along with a dimeric phosphine-free complex (see more below). For polymerization control experiments, mononuclear complexes **FI-**

Ni-A and **FI-Ni-B** were synthesized via reaction of the corresponding monosalicylaldiminate sodium salt[11] with the aforementioned Ni(II) precursors. A monometallic control complex with one Ni site replaced by a bulky TMS group was prepared by reaction of 1.0 equiv of the Ni(II) precursor with the disodium salt of **FI^2-H$_2$**, followed by addition of TMS-Cl in situ to yield **FI^2(TMS)-Ni** (Scheme 1). Stepwise Ni incorporation was then monitored by integration of the now inequivalent *i*-propyl and imine ^{1}H NMR resonances. This monometallic complex was designed to probe the nature and extent of Ni···Ni cooperativity effects on polymerization and to verify that the effects observed are not the result of simple steric crowding, but are due to the presence of two active metal sites.

In the course of **FI^2-Ni$_2$-A/B** crystal growth attempts, long-term experiments yielded two unique systems. Crystals suitable for X-ray crystallographic analysis of dimeric **(FI^2-Ni)$_2$** and the monophosphine derivative **(FI^2-Ni$_2$PMe$_3$)·PMe$_3$** were obtained by slow diffusion of hexane into an ether solution of complex **FI^2-Ni$_2$-A**. In the former complex, each Ni is coordinated to two FI^2 ligands in an approximately square planar arrangement with a *trans-O$_3$N* disposition of the donor atoms. In addition, the phenolate oxygen atoms (O1 and O1′) bridge both Ni atoms (Figure 1). Note that one N ligand of each FI^2 group remains uncoordinated, and is detected as an inequivalent imine signal in the ^{1}H NMR. Important metrical parameters for **(FI^{2}Ni)$_2$** and **(FI^2-Ni$_2$PMe$_3$)·PMe$_3$** are collected in Table 2. The μ-O bridge in **(FI^{2}Ni)$_2$** gives rise to a distorted Ni_2O_2 metallocycle, with a Ni1···Ni1' separation of 2.992(9). This dimeric structure is clearly the result of phosphine dissociation and subsequent ligand redistribution of two **FI^2-Ni$_2$** molecules. The resultant dimer is catalytically inactive due to the absence of a free coordination site and is of a type well documented in the literature,[8d,11] several of which are derived from redistribution of monometallic polymerization catalysts, an example of which is shown in **F**.[11e]

F

From the data in Table 2 it can be seen that the phenolate μ-O ligands are not symmetrically bound (Ni1-O1 = 1.969(1) Å, Ni1′-O1 = 1.659(7) Å). The Ni−O (nonbridging) and Ni−N (nonbridging) distances of 1.969(3) and 1.699(1) Å, respectively, are unexceptional, and can be compared to Ni-O and Ni-N distances of 1.834(3) and 1.949(3), respectively, in **F**.[11]

The Ni coordination geometries in **(FI^2-Ni$_2$PMe$_3$)·PMe$_3$** are essentially square-planar but are bound unsymmetrically to the FI^2 ligand as in **(FI^{2}Ni)$_2$** above, with Ni1 coordinated to two phenolate O atoms (one bridging, one not), and Ni2 coordinated to a bridging phenolate O atom and an imino N atom (Figure 2). The Ni···Ni distance of 3.092(3) Å in **(FI^2-Ni$_2$PMe$_3$)·PMe$_3$** is slightly longer than that in **(FI^{2}Ni)$_2$** (~0.1 Å), possibly reflecting the greater steric demands of the μ-PMe$_3$ ligand. Each Ni is bound to a single methyl group, with the slight differences in Ni-C distances, Ni1-C30 = 1.905(6) Å and Ni2−C31 = 1.932(2) Å, attributable to the different Ni coordination environments. The present Ni-O (bridging) distances of 2.014(1) and 2.021(1) Å are slightly longer than those in **(FI^{2}Ni)$_2$**, and the bonding is more symmetrical. The Ni-O (nonbridging) distance of 1.965(2) Å is comparable to those in **(FI^{2}Ni)$_2$** while the Ni-N distance of 1.723(4) Å is somewhat longer than that in **(FI^{2}Ni)$_2$**, 1.599(1) Å, but not exceptional. The PMe$_3$ ligand in **(FI^2-Ni$_2$PMe$_3$)·PMe$_3$** is bound in an unusual but not completely unprecedented[18] μ-PMe$_3$ mode. The Ni-PMe$_3$ coordination is slightly unsymmetrical with Ni1-P1 and Ni2-P1 = 2.376(6) and 2.392(9) Å, respectively. The geometry about P is shown in **G**, with Ni1-P1-Ni2 = 68.2(2)°, C27-P1-C29 = 102.9(5)°, C28-P1-C29 = 101.8(3)°, and C27-P1-C28 = 98.1(2). Interestingly, the P-C bond lengths of 1.822(4), 1.815(3) and 1.826(4) Å are only slightly shorter than those of free PMe$_3$, which has P-C bond lengths of 1.843 Å.[18b] This type of μ-PR$_3$ coordination has precedent in a number of metal cluster structures in the literature,[18] such as in **H**. Only trace quantities of **(FI^2-Ni$_2$PMe$_3$)·PMe$_3$** could be isolated, and detailed spectroscopic characterization was not possible. ^{31}P NMR resonances attributable to μ-P(alkyl)$_3$ species[18a,b] were not observed in the **FI^2-Ni$_2$-A → (FI^{2}Ni)$_2$** conversion described above.

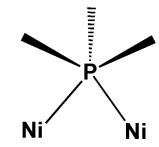

G

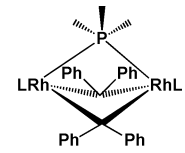

H

Note that the crystallographically defined metal−ligand arrays in both **(FI^{2}Ni)$_2$** and **(FI^2-Ni$_2$PMe$_3$)·PMe$_3$** are substantially less

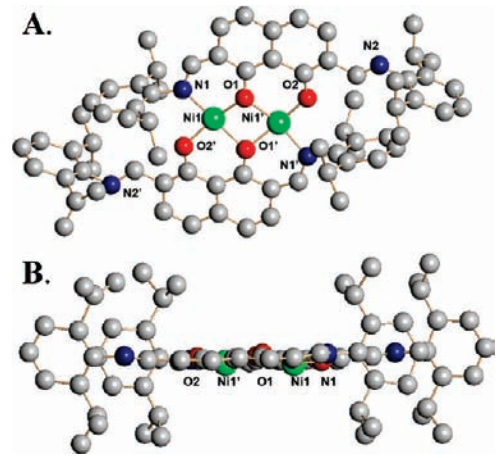

Figure 1. Plot of the molecular structure of the **FI^2-Ni$_2$-A** thermoylsis product, **(FI^{2}Ni)$_2$**. (A.) View perpendicular to the molecular plane. (B.) View in the molecular plane. H atoms are omitted for clarity, as is a lattice Et_2O molecule. Symmetry transformation used to generate equivalent atoms: ′ = $-x,-y,-z$.

(18) (a) Kabir, S. E.; Saha, M. S.; Tocher, D. A.; Hossain, G. M. G.; Rosenberg, E. *J. Organomet. Chem.* **2006**, *691*, 97–104. (b) Pechmnn, T.; Brandt, C. D; Werner, H. *Chem. Eur. J.* **2004**, *10*, 728–736. (c) Pechmnn, T.; Brandt, C. D; Werner, H. *Angew. Chem., Int. Ed.* **2002**, *41*, 2301–2303. (d) Pechmnn, T.; Brandt, C. D; Werner, H. *Angew. Chem., Int. Ed.* **2000**, *39*, 3909–3911. (e) Bruce, M. I.; Hinchliffe, J. R.; Surynt, R.; Skelton, B. W.; White, A. H. *J. Organomet. Chem.* **1994**, *469*, 89–97. (f) Karsch, H. H.; Deubelly, B.; Müller, G. *J. Organomet. Chem.* **1988**, *352*, 47–59. (g) Karsh, H. H.; Appelt, A.; Deubelly, B.; Müller, G. *J. Chem. Soc., Chem. Commun.* **1987**, 1033–1034.

Table 2. Selected bond distances [Å] and angles [deg] for **$(FI^2Ni)_2$** and **$(FI^2\text{-}Ni_2PMe_3)\cdot PMe_3$**

$(FI^2Ni)_2$				$(FI^2\text{-}Ni_2PMe_3)\cdot PMe_3$			
C1-O1	1.421(4)	Ni1-O2′	1.969(3)	Ni1-O1	1.965(2)	Ni1-P1	2.476(6)
C3-O2	1.429(2)	Ni1′-O1	1.659(7)	Ni1-O2	2.014(1)	Ni2-P1	2.392(9)
C11-N1	1.394(6)	Ni1-O1	1.969(1)	Ni2-O2	2.021(1)	Ni1···Ni2	3.092(3)
C12-N2	1.480(3)			Ni2-N1	1.723(4)	P1-C27	1.822(4)
N1-Ni1	1.699(1)	Ni1···Ni1′	2.992(9)	Ni1-C30	1.905(6)	P1-C28	1.815(3)
Ni1′-O2	1.659(2)			Ni2-C31	1.932(2)	P1-C29	1.836(4)
				Ni1-P1-Ni2	68.2(2)	C27-P1-C28	98.1(2)
O1-Ni1-O2	89.9(8)	N1-Ni1′-O1	89.9(8)	P1-Ni1-C30	82.3(1)	C27-P1-C29	102.9(5)
O1-Ni1-O1′	95.3(5)	N1-Ni1′-O2′	103.7(5)	N1-Ni2-O2	90.2(0)	C28-P1-C29	101.8(3)
Ni1-O1-Ni1′	109.1(9)			O1-Ni1-O2	90.4(2)	P1-Ni2-N1	81.6(4)
				P1-Ni2-N1	171.6(7)	P1-Ni1-O2	94.5(1)

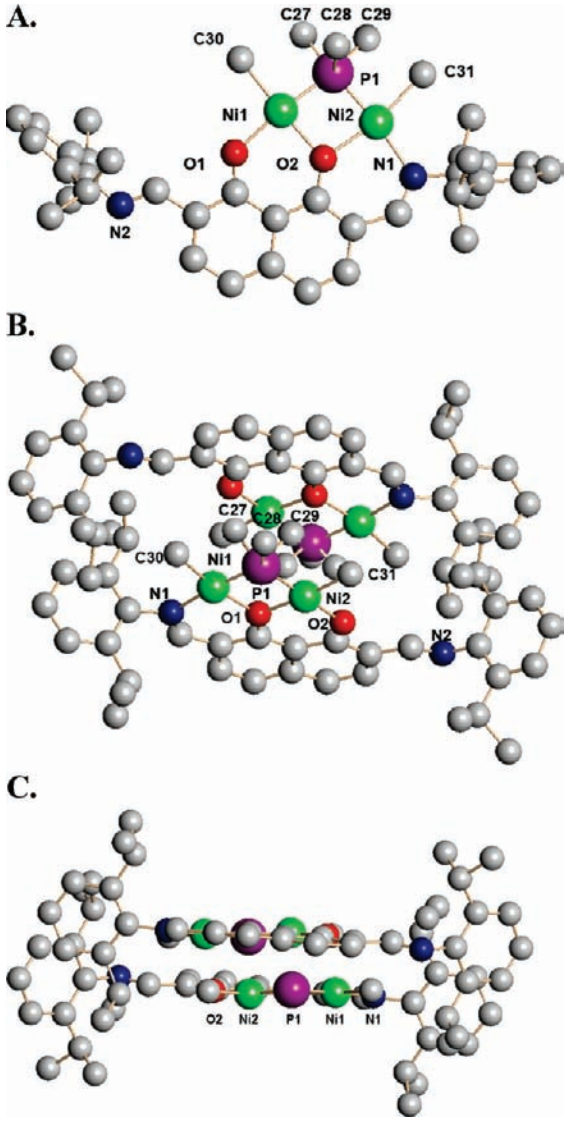

Figure 2. Plot of the molecular structure of monophosphine derivative **$(FI^2\text{-}Ni_2PMe_3)\cdot PMe_3$**. (A) View perpendicular to the molecular plane. (B) View showing molecular stacking in the unit cell. (C) View in the molecular plane showing stacking in the unit cell. H atoms are omitted for clarity, as are lattice Et_2O and PMe_3 molecules. Plane and symmetry transformation used to generate equivalent atoms: $' = -x, -y, -z$ In (C), the P-Me groups are also omitted to allow for viewing of the molecular planarity.

symmetrical than the approximately C_{2v} geometries established for **$FI^2\text{-}Ni_2$-A** and **$FI^2\text{-}Ni_2$-B** on the basis of 1-D ^{1}H, ^{13}C, ^{31}P, and 2-D COSY and NOESY NMR spectroscopy (Chart 2). In both crystal structures, the intramolecular Ni···Ni distance is shorter than the sum of the Ni atomic van der Waals radii (3.3 Å), and may allow chemically significant interactions.[19]

3.2. Polymerization Experiments and Polymer Characterization. General Remarks. All olefin polymerizations were performed as described in the Experimental Section. Polymeric products were characterized by ^{1}H and ^{13}C NMR spectroscopy, gel permeation chromatography, FT-IR spectroscopy, and differential scanning calorimetry as required. To determine the density of alkyl group branching in polyethylene homo- and copolymers, integration of the ^{1}H NMR spectra yields the relative density of methyl and other groups versus the polymer backbone resonances.[15] For other copolymerizations, the comonomer incorporation density is determined by integration of the ^{13}C NMR spectra using standard procedures.[15] Characterization of the ethylene + acrylate copolymerization products included NMR spectroscopy (^{1}H, ^{13}C, and ^{1}H-^{1}H COSY) and DSC to differentiate copolymers from simple physical mixtures. Similarly, both the copolymers and representative physical mixtures were subjected to selective solvent extraction experiments to verify that a heterogeneous polyethylene + polyacrylate physical mixture could be cleanly separated, while a random ethylene + acrylate copolymer would remain homogeneous. Furthermore, GPC with UV detection was also performed in addition to GPC with RI detection to allow more accurate detection of acrylate containing polymers.[13e−j,20] Utilizing both refractive index and ultraviolet GPC detection aids in differentiating mixtures of homopolymers from acrylate-containing random copolymers.

3.3. Ethylene Homopolymerization Experiments. Room temperature ethylene homopolymerizations using the present catalysts were carried out in the presence of the phosphine scavenger/cocatalyst $Ni(cod)_2$ under conditions minimizing mass transport and exotherm effects.[3,4] It can be seen in Table 3 that bimetallic **$FI^2\text{-}Ni_2$-A** and **$FI^2\text{-}Ni_2$-B** catalysts afford polyethylenes with molecular weights comparable to those produced by the analogous monometallic **FI-Ni_1-A**, **FI-Ni_1-B**, and **FI^2(TMS)-Ni_1** controls, having polydispersities consistent with single-site processes. Note however that the bimetallic catalysts exhibit an approximately 2-fold greater polymerization activity along with increased methyl branch density. The branch density assayed by ^{1}H NMR[15] is ∼2× that achieved by the mononuclear catalysts under identical reaction conditions, with the greater branch density also supported by depressed DSC-determined

(19) Soldatov, D. V; Henegouwen, A. T; Enright, G. D; Ratcliffe, C. I; Ripmeester, J. A. *Inorg. Chem.* **2001**, *40*, 1626–1636, and references therein.

(20) (a) Diaz-Requejo, M.; Werhmann, P.; Leatherman, M. D.; Trofimenko, S.; Mecking, S; Brookhart, M.; Perez, P. J *Macromolecules* **2005**, *38*, 4966–4969. (b) Stibrany, R. T.; Schulz, D. N.; Kacker, S.; Patil, A. O.; Baugh, L. S.; Rucker, S. P.; Zushma, S.; Berluche, E.; Sissano, J. A. *Macromolecules* **2003**, *36*, 8584–8586. (c) Johnson, L. K.; Mecking, S.; Brookhart, M. *J. Am. Chem. Soc.* **1996**, *118*, 267–268.

Table 3. Ethylene Homopolymerization Data with and without $Ni(cod)_2$ Cocatalyst Using Mono- and Binuclear Ni-Aryloxyiminato Catalysts

entry	catalyst	cocatalyst	polymer yield (g)	polymer M_w[a]	polymer M_w/M_n	branches/ 1000C[b]	T_m °C[c]	activity[d]
1	**FI^2-Ni_2-A**[e]	$Ni(cod)_2$	0.663	10300	2.6	80	68	7.1
2	**FI^2-Ni_2-B**[e]	$Ni(cod)_2$	0.684	10100	2.6	93	66	7.4
3	**FI^2-Ni_2-B**[f]	$Ni(cod)_2$	0.631	10700	2.6	92	68	6.8
4	**FI^2-Ni_2-B**[g]	$Ni(cod)_2$	0.566	10900	2.6	86	68	6.2
5	**FI-Ni-A**[e]	$Ni(cod)_2$	0.167	11700	2.5	52	93	3.6
6	**FI-Ni-B**[e]	$Ni(cod)_2$	0.175	10500	2.5	54	97	3.7
7	**FI^2(TMS)-Ni**[e]	$Ni(cod)_2$	0.141	11200	2.6	40	98	3.3
8	**FI^2-Ni_2-A**[h]	–	0.103	6000	2.7	102	60	0.2
9	**FI^2-Ni_2-B**[h]	–	0.196	7000	2.7	105	61	0.4
10	**FI-Ni-A**[h]	–	i	–	–	–	–	–
11	**FI-Ni-B**[h]	–	i	–	–	–	–	

[a] Determined by GPC vs polyethylene standards, uncorrected. [b] Determined by ^1H NMR. [c] Melting temperature determined by DSC. [d] Kilograms of polyethylene/ (mol Ni·h·atm). [e] Polymerizations carried out with 10 μmol catalyst and 2.0 equiv of cocatalyst/Ni center at 25 °C for 40 min in 25 mL of toluene at 7.0 atm ethylene pressure. [f] Polymerizations carried out with 10 μmol catalyst and 2.0 equiv of cocatalyst/Ni at 25 °C for 60 min in 25 mL of toluene at 7.0 atm ethylene. [g] Polymerizations carried out with 10 μmol catalyst and 2.0 equiv of cocatalyst/Ni at 25 °C for 90 min in 25 mL of of toluene at 7.0 atm ethylene. [h] Polymerizations carried out with 20 μmol of catalyst at 25 °C for 2 h in 25 mL of toluene at 7.0 atm ethylene. [i] Negligible polymer obtained.

melting points. Interestingly, no branches longer than methyl are detected under these reaction conditions in the **FI^2-Ni_2**-mediated polymerization products. The polymerizations mediated by the PMe_3 and PPh_3-containing catalysts exhibit similar activities, regardless of the phosphine, reflecting the role of the $Ni(cod)_2$ cocatalyst as an effective phosphine-abstracting "sponge".[8−11] When no cocatalyst is used in the bimetallic polymerizations, modest activity is still exhibited, presumably due to nonbonded repulsions of the proximate phosphine groups, favoring dissociation and catalyst self-activation. This is further evidenced in the crystal structure of **(FI^2-Ni_2PMe_3)·PMe_3** discussed above, which illustrates the tendency for phosphine dissociation. Not surprisingly, this effect is slightly more pronounced in the PPh_3 complex than in the PMe_3 analogue (compare Table 3, entries 8 and 9). In contrast, negligible catalytic activity is observed with the monometallic catalysts in the absence of the phosphine-abstracting cocatalyst. Attempts to conduct polymerizations with the bimetallic catalysts at higher temperatures yield negligible polyolefin product and formation of coordinatively saturated **(FI^2-Ni)$_2$** species, one of which was characterized by single-crystal X-ray diffraction, as described above. This result is reminiscent of the Ni dimers reported by Grubbs et al.[11d] and Brookhart et al.[13e] for other classes of mononuclear Ni catalysts. Furthermore, variable-temperature ^{31}P NMR spectroscopy was performed on the present binuclear catalyst solutions to examine the phosphine dissociation characteristics of **FI^2-Ni_2-A** and **FI^2-Ni_2-B.** On warming solutions of **FI^2-Ni_2-B** from 25 to 35 °C, a free triphenylphosphine signal is observed at $\delta = 4$ ppm in addition to that for **FI^2-Ni_2-B**, the intensity of which declines as the free PPh_3 resonance grows in. No other ^{31}P resonances are observed. Furthermore, cooling the solution back to room temperature does not result in recoordination of the free phosphine to the Ni centers (See Supporting Information).

3.4. Ethylene Homopolymerizations as a Function of Ethylene Pressure. One distinctive characteristic of the **FI^2-Ni_2** catalysts is the nearly exclusive formation of methyl branches under our standard reaction conditions (7.0 atm ethylene), while significant densities of longer branching are produced in the present monometallic control experiments, as well as with monometallic catalysts investigated by other groups.[10−13,16] As has been previously shown regarding branch formation in other Ni(II)-mediated polymerization processes, the degree and length of branching obtained is highly dependent on the ethylene concentration during the polymerization,[13] a consequence of so-called "chain-walking" processes[8] (Scheme 2) in which incoming monomer activation/enchainment (k_{insert}) competes with β-H elimination/isomerization (k_{elim}). To determine whether similar processes are operative in the present bimetallic systems, polymerizations were carried out over a range of ethylene pressures. As shown in Table 4 and Figure 3, when the ethylene pressure is increased from 3.0 atm to 5.0 to 7.0 atm, ^{13}C signals representative of ethyl branching are suppressed. Polymerizations carried out with the present monometallic catalysts parallel previously reported trends[8d] in polyethylene microstructure, as do the **FI^2-Ni_2** bimetallic systems, with an approximate proportionality between ethylene concentration and polymerization activity, and suppression of branch formation with increasing ethylene concentration. Note in Figure 3 the relative intensities of the signals corresponding to the α, β, and γ carbons proximate to a methyl branch compared to the polyethylene backbone. These results are in agreement with the pressure dependence trends observed previously by Brookhart.[8d] Long branches are the result of the competing rates of ethylene coordination/insertion versus Ni-alkyl isomerization, where long branches are formed via multiple chain-walks prior to olefin insertion (Scheme 2). In the case of the bimetallic catalyst systems, no more than one isomerization takes place under these conditions (See Discussion section for additional remarks).

3.5. Ethylene Homopolymerizations in Presence of Polar Additives. Previous work has shown that in the presence of polar cosolvents such as water, the Ni(II) phenoxyiminato catalysts exhibit ethylene polymerization activity, but it is severely diminished, as are branch densities.[11] In view of the bimetallic vs monometallic catalyst enchainment selectivity differences identified above, it was of interest to investigate the polymerization characteristics of the **FI^2-Ni_2** systems versus their **FI-Ni_1** analogues in the presence of 1500 equiv of various polar additives. Thus, ethylene homopolymerizations were carried out in toluene solutions containing polar additives. As shown in Figure 4 and Table 5, polymerization activities decline in the order, toluene > diethyl ether > acetone > water. While the polar additives significantly reduce polymerization activity, it can be seen that the binuclear catalysts remain ~ 3x more active than the mononuclear analogues and achieve far greater branch densities (~6 × for Table 5 entry 2 vs 4). Note also that polymer molecular weights are greatly increased as the polarity of the cosolvent is increased, both in the case of the monometallic and bimetallic catalysts.

3.6. Ethylene−Norbornene Copolymerizations. As alluded to in the introduction, norbornene incorporation in mononuclear Ni(II)-catalyzed ethylene copolymerizations is possible but at very low levels. To investigate the comonomer enchainment selectivity of the new **FI^2-Ni_2** catalysts, ethylene + norbornene copolymerizations were investigated with the present mono and bimetallic catalysts, using a diversity of norbornenes bearing polar substituents (Figure 5). It is found that modest comonomer enchainment levels are achieved with the present monometallic **FI-Ni_1** catalysts (Table 6), in accord with the results reported for comparable mononuclear catalysts systems.[11e] In marked

Scheme 2. Chain-Walking Mechanism in Ethylene Polymerizations

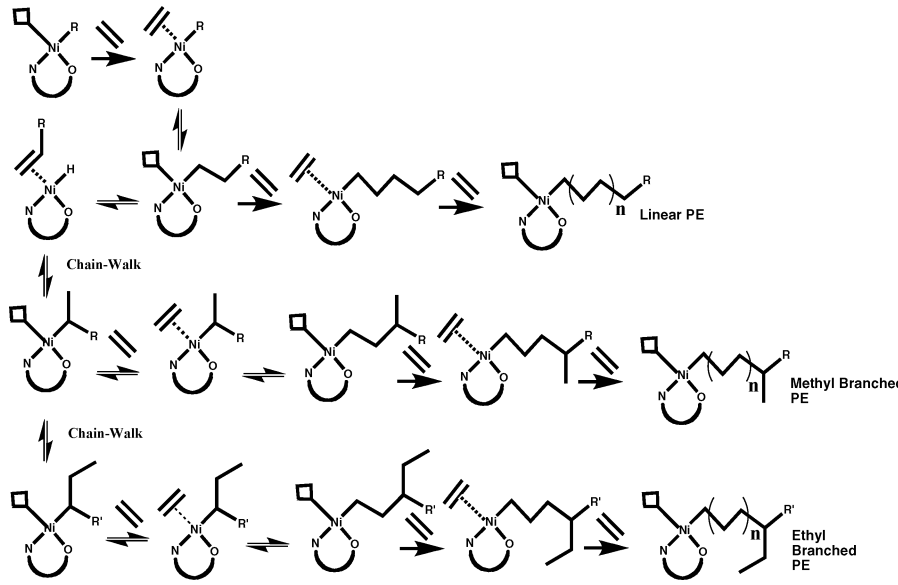

Table 4. Ethylene Homopolymerization Data at Varying Ethylene Pressures Mediated by Mono- and Binuclear Ni Phenoxyiminato Catalysts

entry	catalyst[a]	*P* (atm)	polymer yield (g)	activity[b]	M_w[c]	M_w/M_n	T_m °C[d]	branches/ 1000C[e]
1	**FI^2-Ni$_2$-A**	3.0	0.113	7.5	8400	2.4	52	107
2	**FI-Ni-A**	3.0	0.027	3.9	8200	2.5	88	71
3	**FI^2-Ni$_2$-B**	3.0	0.108	7.2	8200	2.5	53	115
4	**FI-Ni-B**	3.0	0.022	3.9	7900	2.5	82	68
5	**FI^2-Ni$_2$-A**	5.0	0.292	19.7	9200	2.4	64	99
6	**FI-Ni-A**	5.0	0.070	10.5	9100	2.6	92	62
7	**FI^2-Ni$_2$-B**	5.0	0.286	19.7	9700	2.4	66	101
8	**FI-Ni-B**	5.0	0.069	10.0	9600	2.5	91	66
9	**FI^2-Ni$_2$-A**	7.0	0.703	46.9	10100	2.6	68	80
10	**FI-Ni-A**	7.0	0.167	25.2	11700	2.5	93	52
11	**FI^2-Ni$_2$-B**	7.0	0.711	47.6	10000	2.6	68	92
12	**FI-Ni-B**	7.0	0.175	25.6	10500	2.5	97	54

[a] Polymerizations carried out with 10 μmol catalyst and 2.0 equiv of cocatalyst/Ni center at 25 °C for 90 min in 25 mL of toluene. [b] Kilograms of polyethylene/ (mol of Ni·h) Not normalized for pressure to illustrate the change in activity. [c] Determined by GPC vs polyethylene standard, uncorrected. [d] Melting temperature determined by DSC. [e] Determined by ^{1}H NMR.

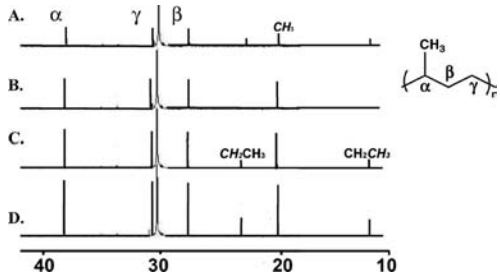

Figure 3. ^{13}C NMR spectra in $CDCl_3$ at 100 MHz of PE polymer produced by (a) monometallic catalyst **FI-Ni** at 7.0 atm, (b) bimetallic catalyst **FI^2-Ni$_2$** at 7.0 atm, (c) 5.0 atm, and (d) 3.0 atm ethylene pressure. Note the increase in relative intensity of branches compared to the polymer backbone resonance with decreasing ethylene concentration. Spectral assignments are as indicated.

contrast, ethylene + norbornene copolymerizations mediated by binuclear **FI^2-Ni$_2$-A** and **FI^2-Ni$_2$-B** proceed with 3−4 × greater activity and with 3−4x greater selectivity for comonomer enchainment than the **FI-Ni$_1$** mediated processes under identical reaction conditions. Note that product molecular weights are comparable to those in the homopolymerization experiments discussed above. Despite somewhat increased polydispersities, both **FI^2-Ni$_2$-A** and **FI^2-Ni$_2$-B** produce polymers with microstructures and with molecular weights similar to those of the monometallic catalysts. Attempts to carry out ethylene copolymerizations in the presence of monomer **NB4** yielded negligible polymeric product. This result likely reflects the acidity of this comonomer, since ^{1}H NMR spectra show that the ligand has been protonated at the hydroxyl functionality.

3.7. Ethylene−Acrylate Copolymerizations. Up to this point, we have focused on exploring whether a second catalytic center might enhance the enchainment characteristics that make neutrally charged monometallic Ni catalytic systems distinctive. However, there are also polar comonomers of interest that are only minimally responsive to the monometallic **FI-Ni** systems, such as methylacrylate or methyl methacrylate. It was therefore of interest to investigate the copolymerization characteristics of the present **FI^2-Ni$_2$** catalysts. Thus, ethylene + methylacrylate (**MA**) and methylmethacrylate (**MMA**) copolymerizations mediated by the **FI^2-Ni$_2$** and **FI-Ni$_1$** catalytic systems were studied in detail. While the present monometallic catalysts coenchain negligible **MA** or **MMA**, as assayed by ^{1}H and ^{13}C NMR spectroscopy, the bimetallic catalysts incorporate up to 11% methacrylate in the polyethylene (Table 7). In both cases, the

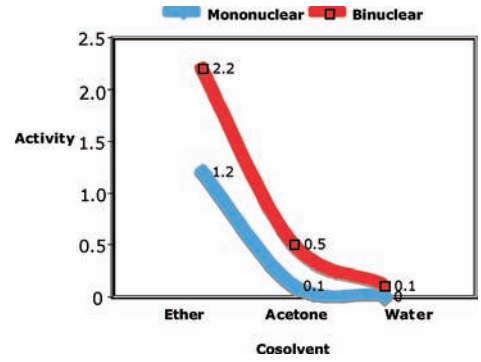

Figure 4. Ethylene polymerization activity in kg PE/mol Ni·h·atm in toluene solution with the indicated cosolvents, mediated by mononuclear (blue) and binuclear (red) Ni phenoxyiminato catalysts.

Table 5. Ethylene Homopolymerization Data in Presence of 5 mol % Polar Additives with Mono- and Bimetallic Ni Catalysts

entry	catalyst[a]	cocatalyst	polar additive	polymer yield (g)	M_w[b]	M_w/M_n	branches/ 1000C[c]	T_m °C[d]	activity[e]
1	**FI^2-Ni$_2$-A**	Ni(cod)$_2$	ethyl ether	0.299	12700	5.4	86	71	2.2
2	**FI^2-Ni$_2$B**	Ni(cod)$_2$	ethyl ether	0.314	13200	5.2	81	72	2.3
3	**FI-Ni-A**	Ni(cod)$_2$	ethyl ether	0.077	12800	2.4	18	98	1.2
4	**FI-Ni-B**	Ni(cod)$_2$	ethyl ether	0.060	12000	2.4	13	98	0.9
5	**FI^2-Ni$_2$-A**	Ni(cod)$_2$	acetone	0.067	20200	5.6	82	80	0.5
6	**FI^2-Ni$_2$-B**	Ni(cod)$_2$	acetone	0.074	21100	5.8	90	78	0.5
7	**FI-Ni-A**	Ni(cod)$_2$	acetone	0.010	21000	2.9	h	122	0.1
8	**FI-Ni-B**	Ni(cod)$_2$	acetone	0.009	19100	2.9	h	122	0.1
9	**FI^2-Ni$_2$-A**	Ni(cod)$_2$	water	*e*	–	–	–	–	–
10	**FI^2-Ni$_2$B**	Ni(cod)$_2$	water	0.036	23700	3.9	39	103	0.3
11	**FI-Ni-A**	Ni(cod)$_2$	water	*e*	–	–	–	–	–
12	**FI-Ni-B**	Ni(cod)$_2$	water	0.006	21800	3.1	*f*	122	0.1

[a] Polymerizations carried out with 10 μmol catalyst and 2.0 equiv of cocatalyst/Ni center at 25 °C and 1500 equiv of polar additive for 40 min in 25 mL of toluene at 7.0 atm ethylene pressure. [b] Determined by GPC vs polyethylene standards, uncorrected. [c] Determined by ^{1}H NMR. [d] Melting temperature determined by DSC. [e] Kilograms of polyethylene/(mol Ni·h·atm). [f] Negligible polymer obtained. [g] Insufficient sample.

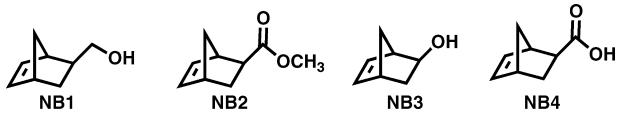

Figure 5. Functionalized norbornenes used as comonomers for ethylene copolymerizations.

copolymers produced yield physical and NMR characteristics similar to random ethylene-acrylate copolymers reported in the literature[21,23] prepared using other transition metal catalysts and/or completely different polymerization pathways (Figure 6). In the present copolymers, the absence of significant ^{13}C NMR resonances at $\delta = 120$ (location a) and 149 (location b) ppm rule out the possibility of significant methylenoate terminated

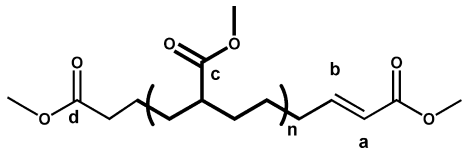

branch end groups.[23d] Furthermore, the location of the copolymer carbonyl resonance at 177 (location c) ppm[23] distinguishes a backbone-incorporated acrylate unit from a branch-capped acrylate (location d) at 176 ppm.[23e] Therefore, essentially all of the MA units incorporated into the copolymer are enchained in the polymer backbone (boldened). In addition, we find that the monometallic catalyst **FI^2(TMS)-Ni** is also incapable of mediating ethylene + acrylate copolymerizations, further supporting a bimetallic enchainment pathway. All product polymer NMR spectra were assigned according to the literature for the products of cationic, monometallic Ni catalysts competent to copolymerize acrylates + ethylene,[23] and are in complete agreement.

Additional selective extraction, GPC, and NMR experiments were conducted to establish that the products of these **FI^2-Ni$_2$**-mediated copolymerizations are indeed random copolymers and not simple physical mixtures of polyethylene and polymethylacrylate or polymethylmethacrylate. These experiments included selective extraction of the copolymers with hot dichloromethane, which at boiling, dissolves both the branched PE and commercially available MMA homopolymers. Upon cooling back to room temperature, the polyethylene PE ($M_w = 21{,}000$; sample of Table 5, entry 6) precipitates out of the concentrated solution, while the PMMA remains dissolved (e.g., $M_w = 120{,}000$). After several washings and repetitions of this extraction process, the results are shown in Figure 7 (^{13}C NMR), which indicate that the physically admixed homopolymers are readily separated by extraction. While these homopolymers could be completely separated, no separation is achieved in the case of the copolymer (see Supporting Information for further data). In addition to the above evidence, the monomodal traces in the RI-detected GPC for the isolated pure PE phase and the pure PMMA extract, in conjunction with the NMR spectra, demonstrate that the physical mixture can be separated. To further distinguish the copolymer from its homopolymer mixture, UV-detected GPC was also performed to determine whether the **FI^2-Ni$_2$**-derived MMA + PE copolymer is monomodal and distinct here from a PMMA homopolymer.[13f–j] As shown in Figure 8, this is the case. DSC was also performed on the MMA + ethylene copolymer and the same physical mixture of homopolymers. As seen in Figure 9, two distinct thermal transitions are observed in the case of the physical mixture, whereas a single transition is evident for the copolymer at 108 °C, in agreement with the literature. Additional copolymer characterization was carried out by IR spectroscopy. The FT-IR spectrum, shown in Figure 10 exhibits characteristic MMA $\nu_{C=O}$ mode at 1738 cm^{-1} and two PE modes at 1480 and 718 cm^{-1}, corresponding to the scissoring and rocking vibrations of the ethylene counits, as assigned for MMA-PE random copolymers.[16,31]

Finally, ^{1}H-^{1}H COSY NMR spectroscopy was performed on both homopolymers and the result compared to that of the ethylene + MMA copolymer. The PMMA homopolymer exhibits no discernible cross-peaks as expected, and the PE spectrum exhibits a single cross-peak indicating branch proton interactions with the backbone protons, as expected (see Supporting Information). In contrast, the ethylene + MMA copolymer exhibits new cross-peaks absent in the homopolymer spectra at $\delta = 1.4$ and 1.8 ppm (Figure 11, circled), corresponding to the proximate enchained acrylate (**A-CH$_2$**) and ethylene units (**PE-CH$_2$**). This crosspeak is relatively weak compared to the **PE-CH$_3$** to **PE-CH$_2$** interaction, since the

(21) (a) Borkar, S.; Yennawar, H.; Sen, A. *Organometallics* **2007**, *26*, 4711–4714. (b) Sen, A.; Borkar, S. *J. Organomet. Chem.* **2007**, *692*, 3291–3299.

(22) Carmona, E.; Marin, Jose, M.; Paneque, M.; Poveda, M. L. *Organometallics* **1987**, *6*, 1757–65.

(23) (a) Skupov, K. M.; Marella, P. R.; Simard, M.; Yap, G. A.; Allen, N.; Conner, D.; Goodall, B. L.; Claverie, J. P. *Macromolecules* **2007**, *28*, 2033–2038. (b) Ydens, I.; Degee, P.; Haddleton, D. M.; Dubois, P. *Eur. Polym. J.* **2005**, *41*, 2255–2263. (c) Elia, C.; Elyashiv-Barad, S.; Sen, A. *Organometallics* **2002**, *21*, 4249–4256. (d) Drent, E.; van Dijk, R.; van Ginkel, R.; van Oort, B.; Pugh, R. I. *Chem. Commun.* **2002**, 744–745. (e) Mecking, S.; Johnson, L. K.; Wang, L.; Brookhart, M. *J. Am. Chem. Soc.* **1998**, *120*, 888–899.

Table 6. Ethylene Copolymerization Data in the Presence of Norbornene (**NB**) and Functionalized Norbornenes **NB1-3** Using Mono- and Bimetallic Ni-Phenoxyiminato Catalysts

entry	catalyst	comonomer	polymer yield (g)	M_w[b]	M_w/M_n	branches/ 1000C[c]	T_m °C[d]	activity[e]	comonomer incorporation[f]
1	**FI^2-Ni$_2$-A**[a]	NB	0.558	66400	5.2	34	107	1.3	9
2	**FI^2-Ni$_2$-B**[a]	NB	0.504	65800	4.5	38	106	1.2	11
3	**FI-Ni-A**[a]	NB	0.072	63200	2.3	9	124	0.3	3
4	**FI-Ni-B**[a]	NB	0.066	64000	2.1	11	124	0.3	3
5	**FI^2-Ni$_2$-A**[a]	NB1	0.488	62600	4.6	39	105	1.2	8
6	**FI^2-Ni$_2$B**[a]	NB1	0.502	63500	4.8	33	109	1.2	9
7	**FI-Ni-A**[a]	NB1	0.067	64900	2.0	9	122	0.3	≤2
8	**FI-Ni-B**[a]	NB1	0.059	63800	2.1	9	122	0.3	3
9	**FI^2-Ni$_2$-A**[a]	NB2	0.444	61800	5.2	33	112	1.1	8
10	**FI^2-Ni$_2$-B**[a]	NB2	0.450	67300	4.8	37	110	1.1	8
11	**FI-Ni-A**[a]	NB2	0.054	65400	2.2	8	122	0.2	≤2
12	**FI-N-B**[a]	NB2	0.058	62000	2.6	8	126	0.3	2
13	**FI^2-Ni$_2$-A**[a]	NB3	0.398	66100	4.4	33	120	0.9	7
14	**FI^2-Ni$_2$-B**[a]	NB3	0.411	64200	4.6	29	112	0.9	8
15	**FI^2-Ni$_2$-A**[a]	NB3	0.029	64100	2.2	8	122	0.1	≤2
16	**FI-Ni-B**[a]	NB3	0.033	62900	2.5	8	124	0.1	≤2

[a] Polymerizations carried out with 10 μmol catalyst and 2.0 equiv of cocatalyst/Ni center at 25 °C and 225 equiv of comonomer for 60 min in 25 mL of toluene at 7.0 atm ethylene pressure. [b] Determined by GPC vs polyethylene standard, uncorrected. [c] Determined by ^{1}H NMR. [d] Melting temperature determined by DSC. [e] Kilograms of polyethylene/(mol Ni·h·atm). [f] Molar percentage determined by ^{13}C NMR.

Table 7. Ethylene Copolymerizations in the Presence of Methylacrylate (**MA**) and Methylmethacrylate (**MMA**)

entry	catalyst[a]	comonomer	polymer yield (g)	M_w[b]	M_w/M_n	alkyl Br/ 1000C[c]	T_m °C[d]	activity[e]	comonomer incorporation[f]
1	**FI^2-Ni$_2$-A**	MMA	0.700	8000	1.4	48	106	1.7	8
2	**FI^2-Ni$_2$-B**	MMA	0.690	7900	1.7	39	106	1.6	9
3	**FI-Ni-A**	MMA	*g*	–	–	–	–	–	–
4	**FI-Ni-B**	MMA	*g*	–	–	–	–	–	–
5	**FI^2-Ni$_2$-A**	MA	0.722	6300	1.6	36	108	1.8	11
6	**FI^2-Ni$_2$-B**	MA	0.741	6700	1.7	37	108	1.8	11
7	**FI-Ni-A**	MA	*g*	–	–	–	–	–	–
8	**FI-Ni-B**	MA	*g*	–	–	–	–	–	–

[a] Polymerizations carried out with 10 μmol catalyst and 2.0 equiv of cocatalyst/Ni center at 25 °C and 225 equiv of polar additive for 60 min in 25 mL of toluene at 7.0 atm ethylene pressure. [b] Determined by GPC vs polyethylene standard, uncorrected. [c] Determined by ^{1}H NMR. [d] Melting temperature (T_m) determined by DSC. [e] Kilograms of polyethylene/ (mol Ni·h·atm). [f] Molar percentage determined by ^{13}C NMR. [g] Negligible polymer obtained.

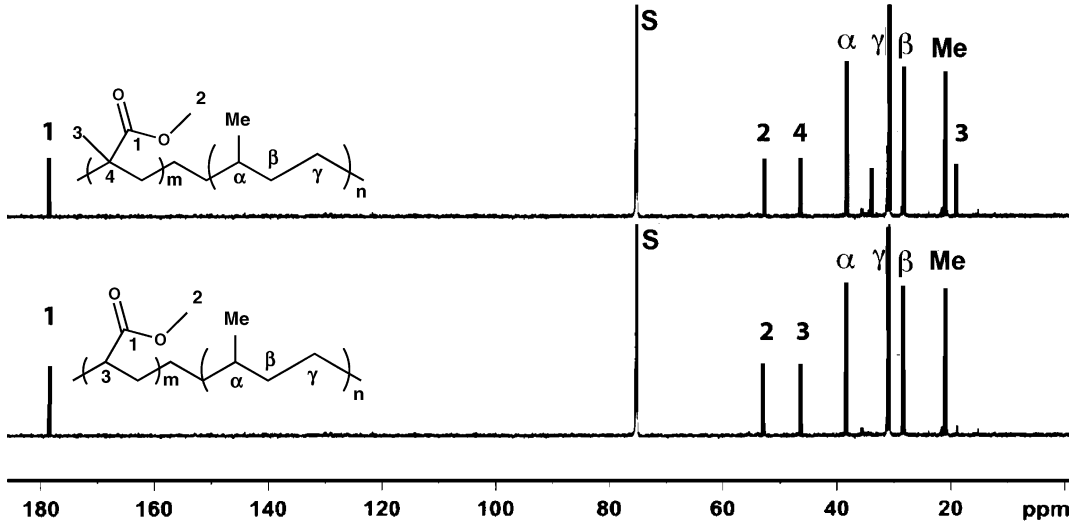

Figure 6. ^{13}C NMR spectra at 100 MHz in $CDCl_3$ of (top) the ethylene + MMA copolymer and (bottom) ethylene + MA copolymer produced by binuclear catalyst **FI^2-Ni$_2$-A.**

copolymer is very highly branched and contains far more methyl branches than enchained acrylate units (the acrylate content is 8%). The results of this experiment, in conjunction with the ^{13}C NMR chemical shift arguments, FT-IR, and DSC data, show definitively that this material is a true copolymer.

3.8. Ethylene−Acrylate Copolymerization Mechanism. With the identity of the **FI^2-Ni$_2$**-derived ethylene + acrylate copolymers confirmed, the next question that arises regards the pathway leading to their formation. To date, the vast majority of group 10 catalysts that produce ethylene + acrylate copolymers are either cationic Ni systems proceeding via a coordinative/insertive pathway, or Pd systems which initiate via a radical pathway.[28] It is therefore important to establish the pathway traversed in the present bimetallic catalysts. To explore the possibility of radical pathways, CH_3OD was employed as a radical trap.[24] In the case of metal complex-mediated radical polymerization, it

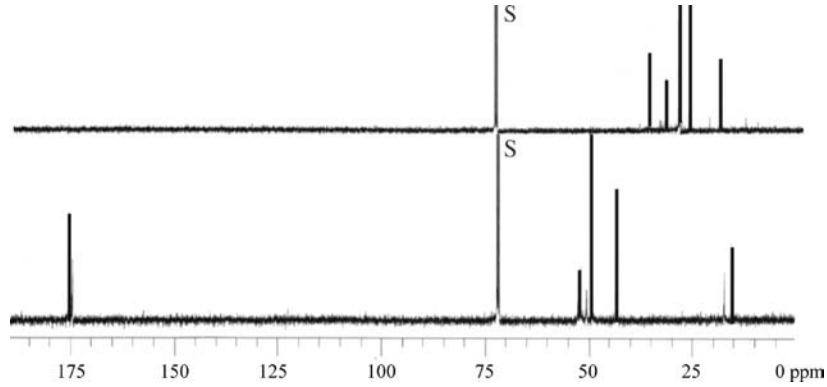

Figure 7. ^{13}C NMR of at 100 MHz in $CDCl_3$ of (top) a highly branched PE insoluble phase and (bottom) commercially available soluble PMMA after repeated extractions of a physical admixture of the homopolymers with CH_2Cl_2. The resulting spectra show complete separation of the homopolymers, as evidenced by the presence or absence of the carbonyl resonance at $d = 175$ ppm and the PE backbone resonance at 30 ppm.

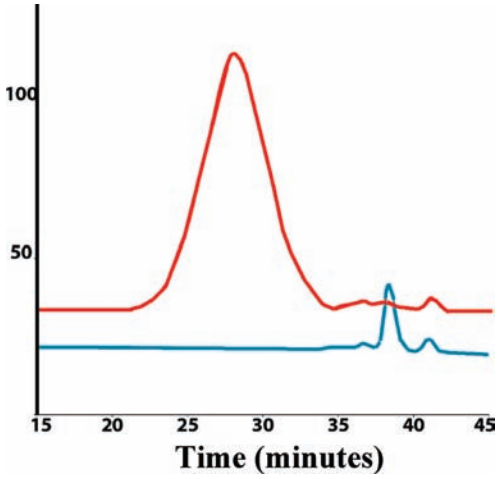

Figure 8. GPC with UV detection at 210 nm of polymer samples of: PMMA homopolymer (red, $M_w = 120{,}000$) and **FI^2-Ni$_2$**- derived ethylene + MMA copolymer (blue, entry 1, Table 7).

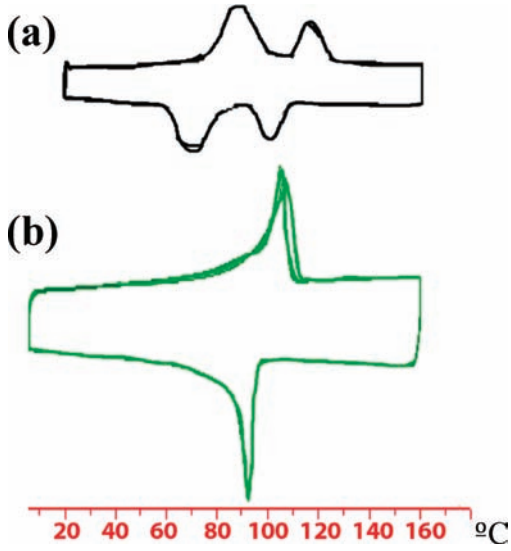

Figure 9. Second scan DSC data for (a) a physical mixture of PMMA and PE homopolymers, (b) the **FI^2-Ni$_2$**-derived ethylene + PMMA copolymer (entry 1, Table 7). Note the single T_g feature obtained for the copolymer as opposed to the distinct individual thermal transitions observed in the polymer mixture.

has been shown that the weaker methanol C−H bond is abstracted by radical species to yield protonated, nonolefinic

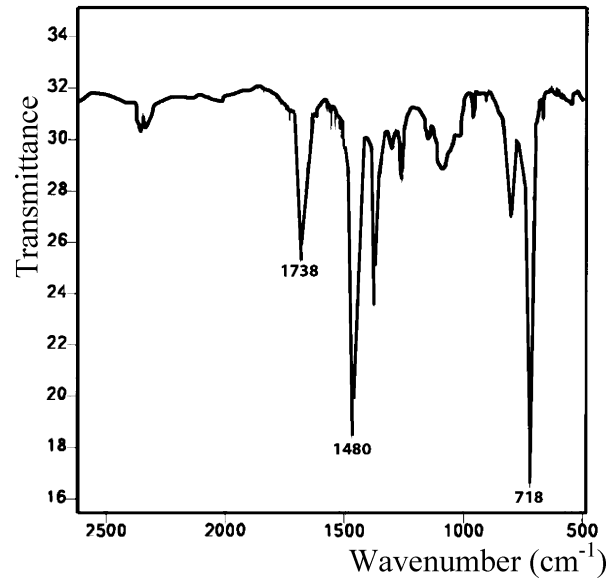

Figure 10. FT-IR spectra of the ethylene + MMA copolymer produced by bimetallic catalyst **FI^2-Ni$_2$** in a KBr pellet. The band at 1738 cm^{-1} corresponds to an inserted MMA unit and two bands at 1480 and 718 cm^{-1} correspond to a polyethylene block.

monomer, whereas for ionic polymerization systems, the more acidic methanol OD is abstracted to yield a deuterated acrylate fragment.[24] In the present case, CH_3OD (0.02 mmol) was added to a solution of **FI^2-Ni$_2$-B** (0.01 mmol), $Ni(cod)_2$ (0.02 mmol), and MMA (0.04 mmol) under an ethylene atmosphere. ^1H and ^2D NMR spectroscopic analysis of the reaction solution shows that the CH_3OD remains unreacted, ruling out the possibility of either predominant cationic or radical copolymerization pathways.

To further probe the nature of the of **FI^2-Ni$_2$**-mediated copolymerization process, ethylene and methylmethacrylate reactivity ratios were determined for the present copolymer formation process. The analysis was performed using the Mayo−Lewis equation[25](eq 1), and compared to published

(24) (a) Hughes, R. P.; Laritchev, R. B.; Zakharov, L. V.; Rheingold, A. L. *Organometallics* **2005**, *24*, 4845–4848. (b) Toscano, P. J.; Brand, H.; Liu, S.; Zubieta, J. *Inorg. Chem.* **1990**, *29*, 2101–2105, and references therein. (c) Kerr, J. A. *Chem Rev.* **1966**, *66*, 465.

(25) (a) Ydens, I.; Degee, P.; Haddleton, D. M.; Dubois, P. *Eur. Polym. J.* **2005**, *41*, 2255–2263. (b) Buback, M.; Dietzsch, H. *Macromol. Chem. Phys.* **2001**, *202*, 1173–1181. (c) Mayo, F. R.; Lewis, F. M. *J. Am. Chem. Soc.* **1944**, *66*, 1594–1601.

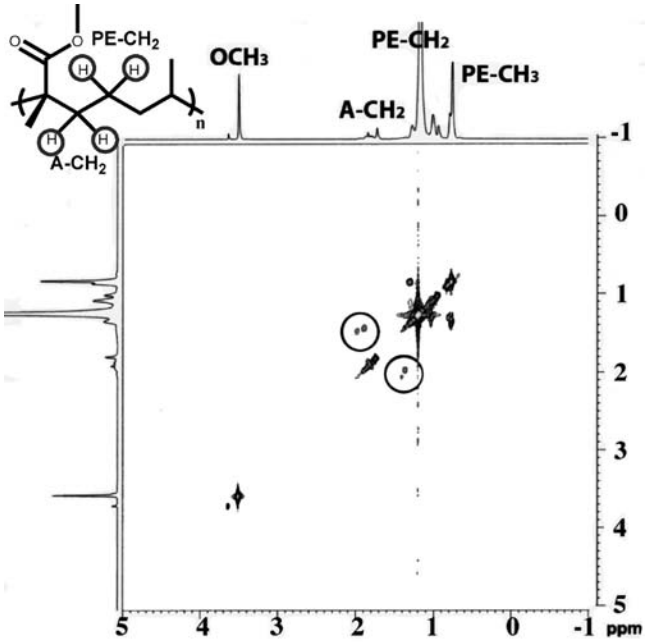

Figure 11. ^{1}H-^{1}H COSY NMR spectrum at 500 MHz in $CDCl_3$ of the PE + MMA copolymer produced by binuclear catalyst **FI^2-Ni$_2$**.

reactivity ratios.[26] In eq 1, dm_i is the mole fraction of monomer i incorporated into the copolymer, M_i is number of moles of monomer i present in the reaction solution, and r_i is the reactivity ratio.

$$\frac{dm_1}{dm_2} = \frac{M_1(r_1M_1 + M_2)}{M_2(r_2M_2 + M_1)} \quad (1)$$

Under the present polymerization reaction conditions, the radical copolymerization of ethylene + MMA should yield $r_{ethylene} = 0.2$ and $r_{mma} = 17$.[26] Calculating the same r values for the **FI^2-Ni$_2$**-mediated copolymerizations, as determined by the NMR assay, yields $r_{ethylene} = 0.34$ and $r_{mma} = 12.2$. Likewise, under the present reaction conditions, the radical copolymerization of ethylene + MA would yield an $r_{ethylene} = 0.2$ and $r_{ma} = 11$.[26] In contrast, the r values for the present **FI^2-Ni$_2$**-mediated copolymerizations, as determined by the NMR assay are $r_{ethylene} = 0.33$ and $r_{ma} = 12.9$. These results argue strongly against significant radical pathway contributions to product formation.

3.9. Low-Temperature Catalyst NMR Studies. In neutral Ni aryloximinato coordinative polymerization catalysts, an agostic interaction can be identified by ^{1}H NMR at low temperatures[8d] involving the vacant Ni coordination site and a β C−H unit on the growing polymer chain (e.g., complex **L**, Scheme 3). It was therefore of interest to determine whether similar agostic interactions take place in the present bimetallic catalysts or whether the presence of a second Ni center may offer additional possibilities. To this end, low temperature ^{1}H NMR studies were undertaken on in situ generated **FI-Ni$_1$** and **FI^2-Ni$_2$** alkyl derivatives. Thus, $NiCl_2(PMe_3)_2$[22] was reacted with the sodium salt of ligand **FI^2-H$_2$**, affording **FI^2-Ni$_2$Cl$_2$(PMe$_3$)$_2$** (complex **M** in Scheme 3). Next, *n*-butyl Grignard was used to generate the very thermally unstable Ni-alkyl species. This solution was rapidly transferred to a cold NMR tube containing $Ni(cod)_2$ and maintained at −20 °C until spectroscopic experiments could be performed. The same procedure was then used to produce an **FI-Ni$_1$** *n*-butyl derivative of the mononuclear Ni catalyst. Note that instead of the *n*-propyl derivative originally investigated by Brookhart in mononuclear anilinotroponate Ni complexes (structure **D** above),[8d] the longer *n*-butyl group was chosen to provide a branch more capable of simultaneously accessing both Ni sites. This choice is supported by molecular modeling studies[30] which indicate that a doubly bound propyl chain would have a C−H···Ni bond length of ∼3.5 Å at lowest energy (Figure 12a), as opposed to a C−H···Ni bond distance of ∼2.8 Å in the analogous butyl species (Figure 12b).

The ^{1}H NMR spectrum of the **FI-Ni$_1$**-butyl complex at −20 °C suggests that *n*-alkyl isomerization has already taken place, similar to that observed by Brookhart, et al.[8d] for *n*-propyl complexes, yielding here complex **L** (Scheme 3) and exhibiting a Ni-CH resonance as a very broad singlet at −2.2 ppm.

Lowering the temperature to −80 °C reveals a broad signal at −9.9 ppm, (see Supporting Information) assignable to a Ni agostic species, similar to that of a previously reported example where Brookhart, et al. installed an *n*-propyl group and observed an agostic signal at −13.9 ppm (**Q**).

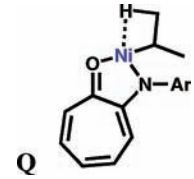

Q

At the same low temperatures, the bimetallic **FI^2-Ni$_2$** dibutyl complex exhibits a similar agostic resonance, as shown in Figure 13. However, solely in the binuclear case is a second resonance is observed at −4.1 ppm. The ^{1}H-^{1}H COSY NMR spectrum of **FI^2-Ni$_2$Bu$_2$** at −80 °C (Figure 14) exhibits two separate alkyl chains-- one chain bound to a Ni participating in no detectable agostic interaction, and another chain participating in two agostic interactions (**P**, Scheme 3). These two alkyl chains can be readily distinguished by the localized interactions between the agostic protons at −4.1 ppm and −9.9 ppm with the protons on the CH_2 between them, at 1.9 ppm, as well as with other proximate protons. The nonagostic chain exhibits a separate group of alkyl proton interactions within the −1.0−1.9 ppm region, which can only be tentatively assigned. Similarly, 1D-TOCSY (see Supporting Information) and ^{1}H-^{13}C HSQC NMR spectroscopy (Figure 15) was also performed on the same bimetallic dibutyl complex. In the TOCSY NMR experiment, the signal assigned to

(26) (a) Brandrup, J., Immergut, E. H., Eds. *Polymer Handbook*, 2nd ed.; John Wiley & Sons, Inc.: New York, 1975. (b) Young, R. J., Ed. *Introduction to Polymers*; Chapman and Hall Ltd.: London, 1981.
(27) (a) Pangborn, A. B.; Giardello, M. A.; Grubbs, R. H.; Rosen, R. K.; Timmers, F. J. *Organometallics* **1996**, *15*, 1518–1520. (b) Klein, H.-F.; Karsch, H. H. *Chem. Ber.* **1973**, *106*, 1433. (c) Van Soolingen, J.; Verkruijsse, H. D.; Keegstra, M. A.; Brandsma, L. *Synth. Commun.* **1990**, *20*, 3153. (d) Salata, M. R.; Marks, T. J. *J. Am. Chem. Soc.* **2008**, *130*, 12.
(28) (a) Tian, G.; Boone, H. W.; Novak, B. M. *Macromolecules* **2001**, *34*, 7656–7663. (b) Elia, C.; Elyashiv-Barad, S.; Sen, A.; Lopez-Fernandez, R.; Albéniz, A. C.; Espinet, P. *Organometallics* **2002**, *21*, 4249–4256. (c) Sen, A.; Borkar, S. *J. Organomet. Chem.* **2007**, *692*, 3291–3299. (d) Kang, M.; Sen, A. *Organometallics* **2005**, *24*, 3508–3515.
(29) Kuptsov, A. H.; Zhizin, G. N. *Handbook of FT Raman and Infrared Spectra of Polymers*; Elsevier: New York, 1998.
(30) *Spartan '06*; Wavefunction, Inc.: Irvine, CA, 2006.
(31) (a) Chen, Q.; Yu, J.; Huang, J. *Organometallics* **2007**, *26*, 617–625. (b) Hu, T.; Tang, L.; Li, X.; Li, Y.; Hu, N. *Organometallics* **2005**, *24*, 2628–2632. (c) Zhang, D.; Jin, G. *Organometallics* **2003**, *22*, 2851–2854. (d) Akitsu, T.; Einaga, Y. *Polyhedron* **2005**, *24*, 1869–1877. (e) Wehrmann, P.; Mecking, S. *Organometallics* **2008**, *27*, 1399–1408, and references therein.

Scheme 3. Synthesis and Possible Agostic Interactions in Model *n*-Butyl Derivatives of Catalysts **FI-Ni$_1$** and **FI^2-Ni$_2$**

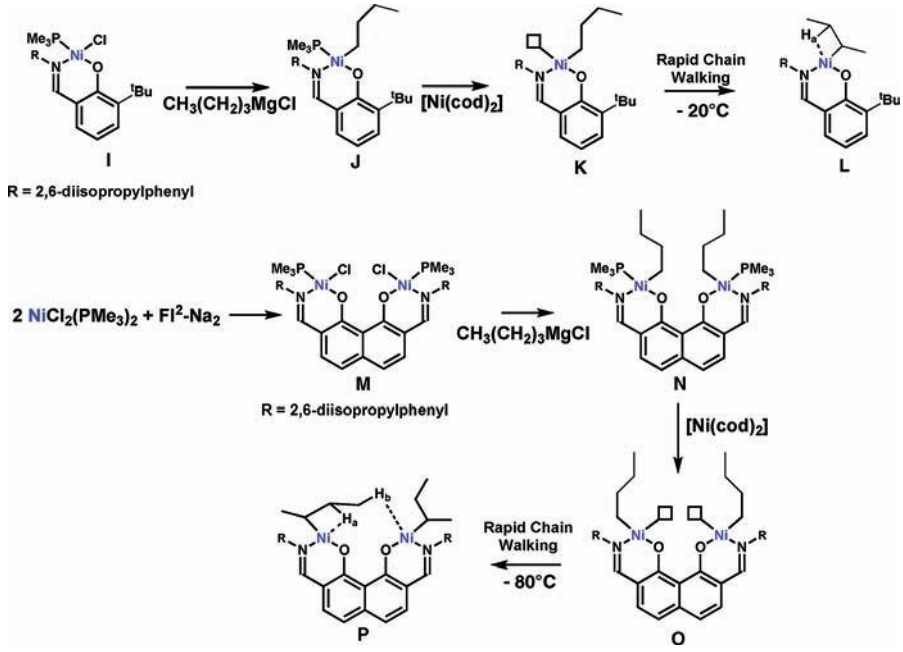

H_a was irradiated. Doing so provides a clearer picture of the signals corresponding to the neighboring protons on the alkyl chain. Most importantly, selectively exciting agostic peak H_a shows a correlation with the second agostic peak, H_b, demonstrating that both protons are on the same alkyl chain. Similarly, the HSQC NMR spectrum shows that one alkyl chain has no agostic proton correlations, while the other has two. This experiment reveals that $^1J(^{13}C-H_a) \approx 85$ Hz and $^1J(^{13}C-H_b) \approx 100$ Hz, which are classic signatures of agostic interactions,[32] with the magnitudes scaling approximately inversely with the upfield shifts.[32]

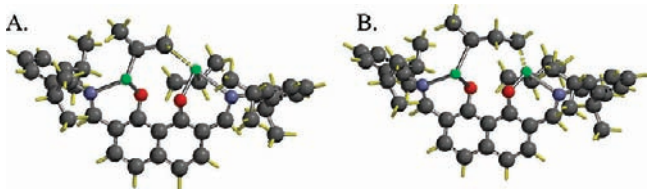

Figure 12. Molecular models of (A.) *i*-propyl branched model compound (Ni-C-H-Ni distance = 3.53 Å) and (B.) *sec*-butyl branched model compound (Ni-C-H-Ni distance = 2.81 Å) showing potential agostic interactions.

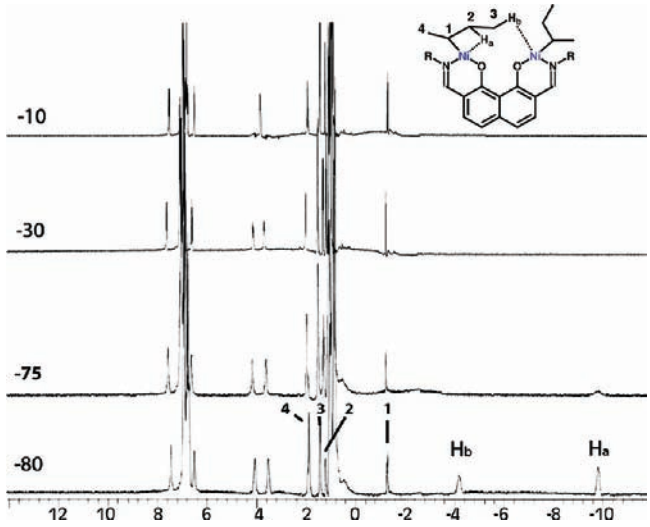

Figure 13. Low-temperature 400 MHz ^{1}H NMR spectra in toluene-d_8 of the bimetallic **FI^2-Ni$_2$** dibutyl complex.

4. Discussion

4.1. Ethylene Homopolymerizations. Comparing the ethylene homopolymerization characteristics of the monometallic **FI-Ni$_1$**- and **FI^2(TMS)-Ni**-derived catalysts with the **FI^2-Ni$_2$**-derived bimetallic systems reveals significant differences that are most plausibly attributed to cooperative effects involving both Ni centers. The **FI^2-Ni$_2$** catalyst activity and product polyethylene branch density determined by ^{1}H NMR[15] are ~2× that achieved by the mononuclear catalysts under identical reaction conditions, and the increased branch density is confirmed by depressed DSC-determined melting points. As noted above, the branching in the **FI^2-Ni$_2$**-derived polyethylenes is more methyl-rich. Moreover, the **FI^2(TMS)-Ni$_1$** polymerization properties show both activity and polymer microstructure similar to that of the present **FI-Ni** and other monometallic catalysts,[8−11] verifying that the increased activity and methyl-rich branch density is exclusive to the **FI^2-Ni$_2$** catalysts bearing a second, adjacent catalytic Ni center. Interestingly, product molecular weights and polydispersities are essentially indistinguishable for the monometallic and bimetallic polymerization systems.

In the absence of a cocatalyst, the present mononuclear systems do not produce significant polyethylene, in agreement with previous observations for similar mononuclear catalysts,[8−10] In contrast, the present bimetallic catalysts produce essentially the same polyethylenes but with increased branch densities and concurrently depressed melting points, albeit at somewhat reduced activities versus the cocatalyzed polymerizations (Table 1, entries 8−11). This particular cocatalyst-related productivity difference between **FI^2-Ni$_2$-A**, **FI^2-Ni$_2$-B**, and the mononuclear

(32) (a) Brookhart, M.; Green, M. L. H.; Parkin, G. *Proc. Natl. Acad. Sci. U.S.A.* **2007**, *104*, 6908–6914, and references therein. (b) Popelier, P. L. A.; Logothetis, G. *J. Organomet. Chem.* **1998**, *555*, 101–111, and references therein.

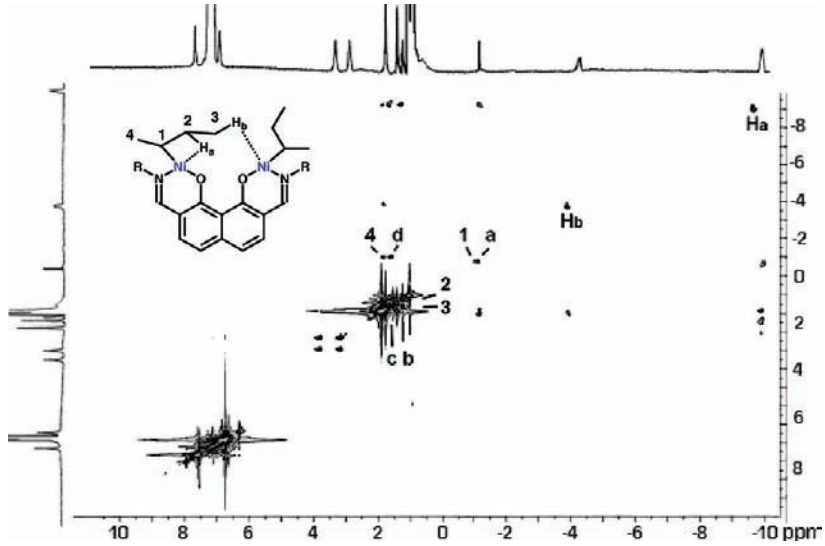

Figure 14. ^{1}H-^{1}H COSY NMR spectrum at 400 MHz at −80 °C in toluene-d_8 of the dibutyl derivative of the bimetallic **FI^2-Ni$_2$** complex.

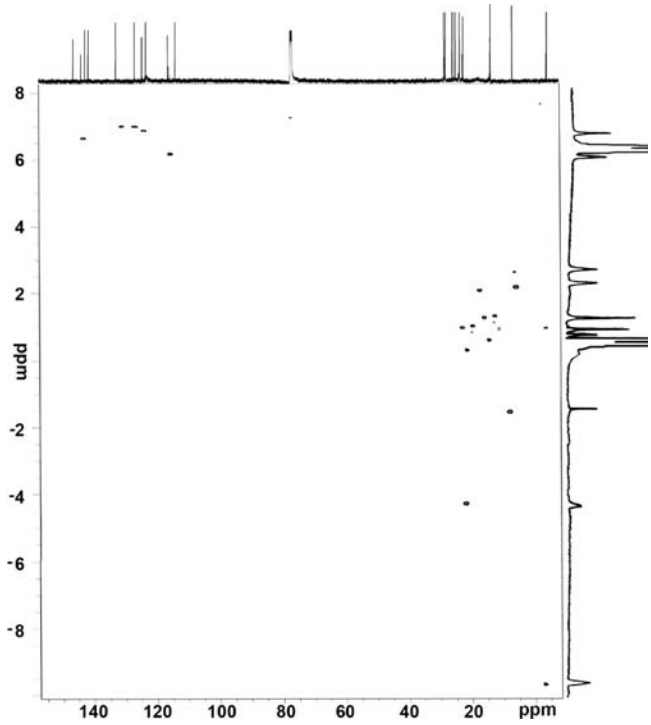

Figure 15. ^{1}H-^{13}C HSQC NMR spectrum at 400 MHz at −80 °C in toluene-d_8 of the bimetallic **FI^2-Ni$_2$** dibutyl complex. $^{1}J(^{13}C-H)$ values of approximately 85 and 100 Hz are determined for H_a and H_b, respectively.

analogues may reflect previously reported phosphine dissociation-related steric and electronic factors.[31] Typically, equilibria between such phosphine-coordinated and uncoordinated species heavily favor the former,[13e] however the proximate bulky phosphine ligands in **FI^2-Ni$_2$-A** and **FI^2-Ni$_2$-B** likely favor phosphine dissociation, as indicated by both ^{31}P NMR and X-ray diffraction results (see above).

The distinctive ethylene homopolymerization characteristics of the **FI^2-Ni$_2$**-based catalysts doubtless reflect a complex interplay of kinetics and thermodynamics. In regard to those factors underlying the relative importance of propagation and chain-walking rates versus the mononuclear analogues, it is clear that any cooperative effects such as enhanced substrate binding/preorganization (e.g., structure **A** above) as proposed for bimetallic group 4 polymerization catalysts,[3,4] do not influence the overall propagation/chain transfer rate ratios in a way that significantly alters the product polyethylene M_w or the polydispersity. However, significant differences in product macromolecule architecture are observed, with higher branch densities and the greater selectivity for methyl branch formation in the **FI^2-Ni$_2$-**mediated homopolymerizations (Tables 3,4; Figure 3) suggesting that the presence of the second Ni center enhances chain walking but suppresses ethyl branch formation versus **FI-Ni$_1$**-mediated processes: (1) by intercepting species such as **R** in Scheme 4 prior to isomerization to species such as **S** (k(PropagationMe)[ethylene] ≫ k(EtBranch), (2) because the equilibrium to form **S** is for steric and/or electronic reasons unfavorable, or (3) because k(PropagationEt)[ethylene] is for steric and/or electronic reasons slower than k(PropagationMe)-[ethylene]. From the low-temperature NMR studies of **FI^2-Ni$_2$Bu$_2$** (Figures 13−15) implicating binuclear agostic interactions, it is conceivable that secondary agostic binding as in structure **T** below may influence the β-H elimination/readdition kinetics of the chain-walking processes, while increased propagation kinetics may reflect monomer binding to the neighboring Ni center, thereby increasing local concentrations.

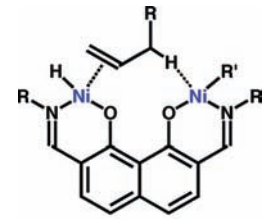

T

The present work also shows that the **FI^2-Ni$_2$-B** catalysts adhere to the same trends in activity and polydispersity as the **FI^2-Ni$_2$-A** analogues: polymerizations exhibit comparable activities between complexes bearing large and small phosphine ligands in all cases, except in the presence of water (Table 5). Note also that, while significant increases in activity and branching are observed for the bimetallic catalysts, the molecular

Scheme 4. Methyl Branch Formation Pathways in **FI²-Ni₂**-Mediated Ethylene Homopolymerization

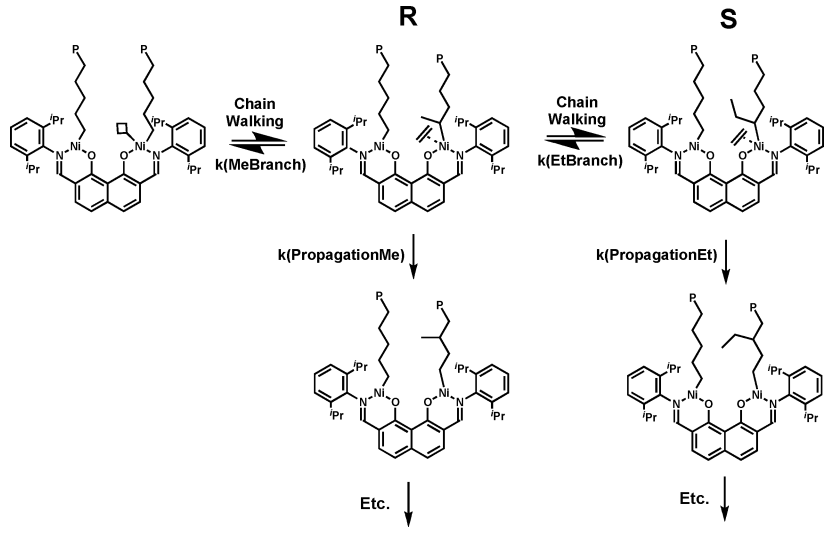

weights of the polyethylene produced by the mono- and binuclear systems are similar.

4.2. Copolymerizations with Polar Comonomers. In copolymerizations with functionalized norbornenes (Figure 5), the present mononuclear catalysts produce copolymers with relatively small levels of polar comonomer incorporation, in agreement with literature results for analogous mononuclear Ni(II) catalysts.[9,10] In marked contrast, the bimetallic **FI²-Ni₂**-derived catalysts exhibit 3−4× enhanced enchainment selectivities and polymerization activities (Table 6) versus the mononuclear analogues, regardless of the polar norbornene substituent, as assayed by NMR spectroscopy. Minimal influence of **NB** polar substituent skeletal position is observed, similar to previous reports with other mononuclear Ni(II) catalysts.[9,10] **FI²-Ni₂-A** and **FI²-Ni₂-B** enchain significant quantities of polar-functionalized norbornene (7−9%) while simultaneously maintaining high methyl branch densities (∼8−10× the level of the mononuclear catalysts) in the oligoethylene blocks. This may be due to rapid reinsertion of the growing polymer at the second metal site after it has undergone elimination by the first.

In the case of ethylene copolymerizations with methylacrylate or methylmethacrylate as comonomers, the present monometallic Ni(II) catalysts are incapable of significant comonomer co-enchainment.[10] However, in the case of the bimetallic **FI²-Ni₂**-derived systems, 8−11% incorporation is achieved to form essentially random acrylate−ethylene copolymers, as determined by NMR spectroscopic assay and other physiochemical measurements. As expected from the ethylene homopolymerizations, once again the **FI²(TMS)-Ni** exhibits reduced activity and minimal polar comonomer enchainment, similar to that of the conventional monometallic phenoxyiminate systems. To explain selectivity for co-enchainment of these previously unresponsive comonomers, we consider the insertion pathway and its potential modification when two metal centers are in close proximity. It has been proposed[10,20] that copolymerization in the mono-nickel polymerization systems is impeded by the formation of a relatively stable/inert six-membered acrylate resting state that occupies the otherwise vacant Ni site used for subsequent ethylene binding/insertion (Scheme 2, Figure 16A). Interestingly, it was recently argued that in the case of styrene polymerizations with monometallic organotitanium CGC catalysts,[3,4] an analogous "back-biting" occurs, in which a styrenic arene group binds to the cationic catalytic Ti center and effectively imepedes monomer approach/activation (Figure 16B). In the case of bimetallic CGC Ti_2 catalytic systems, it was proposed that the styrene π-system is drawn away from one Ti center by the second, proximate Ti electrophile, resulting in far greater monomer access, enhanced propagation rate, and altered insertion regiochemisry.[3e] We suggest that an analogous process is operative in the present bimetallic group 10 systems, wherein a second unsaturated catalytic site abstracts acrylate from the insertion site and thereby facilitates macromolecule propagation subsequent to acrylate activation/enchainment (Figure 16B).

The wide array of macromolecular characterization techniques applied here confirms that the **FI²-Ni₂**-derived ethylene + acrylate copolymers are genuine, essentially random copolymers rather than a physical mixtures of the homopolymers. The copolymers can be differentiated from physical admixtures by DSC, GPC, FT-IR, and selective extraction. Furthermore, ^{1}H-^{1}H COSY NMR experiments evidence distinctive spin−spin interactions within the copolymer structure, not present in the homopolymers, corresponding to neighboring enchained acrylate and ethylene units, evident in Figure 10 as cross-peaks at δ = 1.8 and 1.4 ppm. In addition to ^{1}H-^{1}H COSY NMR evidence that there are no neighboring acrylate units in the copolymer, we suggest that the acrylate incorporation is not exclusively branch-capping, but randomly incorporated into the copolymer backbone. Regarding the position of the ^{13}C NMR carbonyl signal for branch ends versus those within the polymer backbone, the literature reports capped-ends at 176 ppm[23e] and acrylate enchained resonances at 177−178 ppm.[12b,21,23] From Figure 6, the single carbonyl resonance at 178 is assigned as predominately backbone-incorporated from literature data for other ethylene + acrylate random copolymers.[21,23] Furthermore,

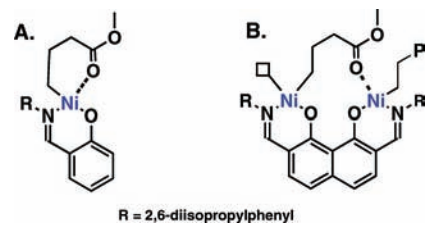

Figure 16. Proposed resting states of mono- and binuclear catalysts after acrylate insertion.

from the ^{1}H and ^{13}C NMR, we have shown that only methyl branches exist. Note that polymerization activities are reduced approximately 4-fold in copolymerizations of acrylate with ethylene compared to ethylene homopolymerizations under the same reaction conditions. While the present density of acrylate incorporation is by no means the highest possible for all transition metal catalysts capable of producing PE + acrylate copolymers under all polymerization conditions,[28] it is the highest, to our knowledge, for all single-site neutrally charged catalytic systems.

4.3. Bimetallic Influence on Olefin Polymerization Pathways. The pathway by which the present bimetallic catalyst olefin enchainment cooperativity effects take place is of central interest in this investigation: What is the nature of the catalytic interaction between the two Ni centers? Radical trapping using CH_3OD was performed to test for radical polymerization pathways, as alternatives to a coordinative polymerization process. The deuterated methanol probe argues that no significant concentrations of radical species are present.[23] However, since radical traps can potentially modify the catalyst under investigation and influence subsequent polymerization pathways,[28a] ethylene + acrylate reactivity ratios were also analyzed for the **FI^2-Ni$_2$**-mediated copolymerizations. For a radical polymerization process, the ethylene + MMA reactivity ratios under the present reaction conditions should be approximately: $r_{ethylene} = 0.2$ and $r_{MMA} = 17$,[26] whereas the experimental values for **FI^2-Ni$_2$**-mediated copolymerizations are: $r_{ethylene} = 0.34$ and $r_{MMA} = 12.2$. For ethylene and MA, a radical copolymerization mechanism would give: $r_{ethylene} = 0.2$ and $r_{MA} = 11$,[26] whereas the measured values for the present copolymerizations are: $r_{ethylene} = 0.33$ and $r_{MA} = 12.9$. In fact, solving for the incorporation ratio ($d_{methylene}/d_{mMMA}$) in the Mayo−Lewis equation for a radical process yields a predicted ethylene/MMA incorporation ratio of 1.7 under the present conditions−far from what is observed. Because the moles of monomer incorporated into the copolymer is known, solving for the expected MMA incorporation were this a radical process under the same reaction conditions yields a predicted MMA incorporation level of over 30 mol %, a value in large excess of that observed in the present copolymer, 9 mol %.

Low temperature 1- and 2D ^{1}H NMR spectroscopy of the thermally labile **FI^2-Ni$_2$Bu$_2$** derivative provides evidence for an agostic species in the bimetallic complex at $\delta = -9.9$ ppm.[8d] However, a second agostic interaction is also observed at $\delta = -4.2$ ppm (Figure 13). The exclusivity of this resonance to the bimetallic system suggests a second agostic interaction of an alkyl group coordinated to one Ni communicating with the second Ni, suggested to be H_b, the γ-proton of a *sec*-Bu ligand (Scheme 3, Figure 13). This observation, in conjunction with the exclusivity of the second peak to the bimetallic complex, also argues against the possibility of an equilibrium between species such as **U** and **V** since this would also be expected in

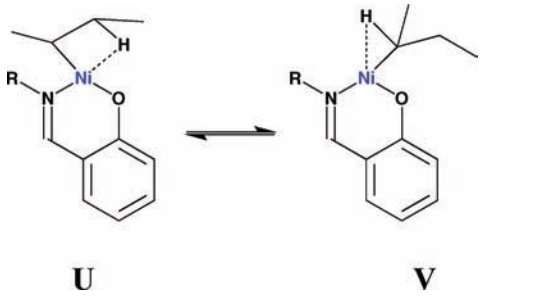

U **V**

the mononuclear complex NMR spectra. Instead the data argue that the second agostic interaction involves a proton from the terminal carbon of the alkyl chain. Warming the NMR tube results in complete degradation of the complex by −10 °C.[8] Furthermore, low-temperature ^{1}H-^{1}H COSY and HSQC NMR spectra (Figures 14 and 15) show definitively that one Ni-alkyl group has no agostic interactions, while another has agostic protons occupying both of the open coordination sites provided by the metal centers. Thus, the agostic proton on the γ C (H_b) shows a cross peak with the protons on the β carbon and with no other. The β agostic proton (H_a) shows two cross peaks, one with the adjacent α C−H at $\delta = -1.6$ ppm and the other with γ C−H at $\delta = 1.5$ ppm. This point is further demonstrated by the $^1J(^{13}C-H)$ coupling constants determined from the ^{13}C NMR obtained in the HSQC experiment, which reveal values of 85 and 100 Hz for H_a and H_b, respectively. These experiments provide strong evidence that the vacant coordination site provided by the second Ni center during polymerizations is structurally/mechanistically communicating with the growing polymer on the first, and that this interaction is crucial for the reported increases polymerization activity and comonomer enchainment selectivity.

Recent complementary binuclear group 10 catalyst studies by Hu, et al.[13b] (**W**) and Mecking, et al.[13d] (**X**), report enhancements in non-cocatalyzed polymerization activity vis-à-vis the mononuclear analogues as well as differences in polyolefin microstructure. The degree to which these observations reflect cooperative effects is not obvious, especially in view of the ligand conformational flexibility and/or the sizable metal−metal distances.[13b,d,31]

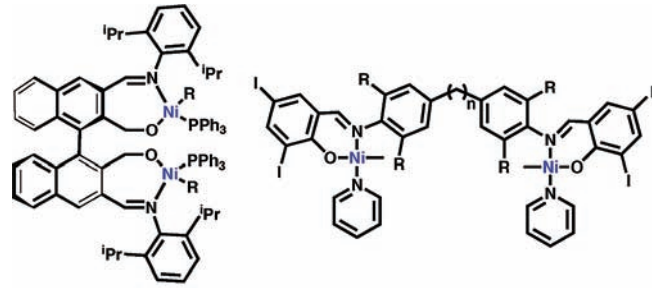

W **X**

5. Conclusions

The synthesis, characterization, and olefin polymerization reactivity of two structurally rigid, neutrally charged bimetallic phenoxyiminato Ni(II) polymerization catalysts and their monometallic analogues is presented. The bimetallic catalysts evidence significant active center−active center cooperative effects in ethylene homopolymerization versus their mononuclear analogues. This cooperativity doubtless reflects the rigid ligation environment that binds the Ni centers in close enough proximity. Evidence for Ni···Ni cooperation includes agostic interactions which span both metal centers. Cooperative bimetallic catalytic interactions are associated with the doubling of the ethylene homopolymerization activity, as well as an increased polar comonomer enchainment selectivity for functionalized norbornenes (4×) and for acrylates (∼10−100×). The selectivity of the bimetallic systems for incorporating higher densities of comonomer, as well as their significantly higher oligo/polyethylene branch content, affords substantially altered polymer microstructures, with lowered melting points and greater solubility. Furthermore, the bimetallic catalysts exhibit significantly higher activities than the monometallic catalysts in the presence of polar solvents, while concurrently achieving higher molecular weights and branch densities. This feature permits

using less rigorously dried media for polymerization while preserving the desired product microstructure. Mechanistic studies confirm that, as in the monometallic species,[8−11] polymerizations follow a coordinative insertion process, with enhanced monomer enchainment facilitated by the second catalytic center.

The point of greatest interest here is not simply the polymerization activities or levels of incorporation alone. It is instead that the cooperative effects evident between group 10 catalytic centers, as shown with the present model complexes, not only afford both substantial enhancements in the catalyst/polymer properties that have made the monometallic analogues of interest but also expand the scope of polymerizations possible.

Acknowledgment. Financial support by DOE under Grant 86ER13511 is acknowledged. M.D. thanks U. of Parma (Italy) for a study leave. We thank Mr. M. Weberski, Jr. for helpful discussions, and Dr. E. Szuromi and Prof. R. F. Jordan (U. of Chicago) for hospitality in GPC measurements.

Supporting Information Available: Details of catalyst synthesis, polymerization experiments, and polymer characterization; NMR spectra of representative polymer samples. This material is available free of charge via the Internet at http://pubs.acs.org.

JA900257K